COMPUTER
METHODS
IN MATERIALS
SCIENCE

2025, vol. 25, no. 4, 5–30
https://doi.org/10.7494/cmms.2025.4.1029

Full-field approaches for austenite-ferrite phase transformation simulations

Mariusz Wermiński*, Mateusz Sitko, Łukasz Madej

AGH University of Krakow, al. A. Mickiewicza 30, 30-059 Krakow, Poland.

Abstract

Understanding the local evolution of phase transformations in steels, particularly the γ (austenite) → α (ferrite) transformation, is crucial for controlling the microstructure and properties of steel components. Over recent decades, significant progress has been made in the numerical modeling of this complex phenomenon. This development has been driven by both scientific curiosity and industrial needs, especially in processes such as hot rolling, forging, thermal treatment, etc. The developed models have evolved from simple solutions based on local equilibrium to more complex approaches that consider local heterogeneities. Modern computational approaches, such as Phase-Field (PF), Level-Set (LS), Cellular Automata (CA), Monte Carlo (MC) or Vertex based simulations, allow for the precise reproduction of microstructural evolution considering local instabilities. They also enable the analysis of phase boundary motion in an explicit manner. These techniques also allow for direct integration with thermodynamic data and mechanical models, thereby better capturing the physical mechanisms of phase transformations, such as chemical composition, diffusion resistance, or the influence of deformation. An overview of the state of the art in this area is presented within the paper. The model's concepts, assumptions, fundamental equations, advantages, limitations, and potential practical applications are summarized. Special attention is given to modeling the γ → α transformation by the Cellular Automata method. The importance of incorporating phenomena such as diffusion, nucleation, and growth is emphasized. The need for consistency between experimental results and simulations is also highlighted.

Keywords: phase transformations, full-field models, austenite, ferrite, cellular automata

1. Introduction

Phase transformations in steels play a key role in shaping their mechanical and physical properties. Particularly important is the transformation of austenite (γ) into ferrite (α), which directly affects the material's microstructure, including the size and shape of grains and the distribution of alloying elements (Bengochea et al., 1998; Furuhara et al., 2008; Wang B. X. et al., 2009). These parameters determine the steel's characteristics, such as hardness, strength, ductility, and impact strength. A theoretical understanding of thermodynamic stability, phase equilibria, or diffusion-driven transformation mechanisms provides the foundation for developing complex thermo-mechanical cycles for new steel grades and tailored products (Hodgson et al., 2005; Zhang Jiantao et al., 2020).

Experimental approaches remain indispensable for studying the evolution of phases within the microstructure during such thermo-mechanical cycles.

---

* Corresponding author
Author's e-mails: marwer@agh.edu.pl, msitko@agh.edu.pl, lmadej@agh.edu.pl
ORCID ID's: 0000-0002-0212-1258 (M. Wermiński), 0000-0003-0893-8784 (M. Sitko), 0000-0003-1032-6963 (Ł. Madej)
Received: 22.09.2025, accepted: 20.10.2025, published: 2.12.2025

Methods such as dilatometry and thermal analysis enable the precise determination of transformation start and finish temperatures, while advanced microscopy techniques – including scanning electron microscopy (SEM), transmission electron microscopy (TEM), and electron backscatter diffraction (EBSD) – allow for the detailed analysis of grain morphology, crystallographic orientation relationships, or phase boundary types (Málek et al., 2020; Ubhi et al., 2014). In-situ techniques, such as synchrotron X-ray diffraction and high-temperature confocal microscopy, offer a real-time observation of phase evolution under controlled conditions (Liang C. et al., 2024; Rozo Vasquez et al., 2023; Zhang Jiantao et al., 2020). Together, these experimental tools provide critical data for calibrating and refining processes in industrial conditions. Besides the enormous possibilities provided by experimental approaches, the time and cost of such analysis are often the main limitations in the development of new processing cycles. Therefore, accurate numerical modeling of phase transformations is crucial to support such experimental investigations at both the material design stage and the optimization of technological processes.

In recent decades, significant progress has been made in numerical modeling of microstructural phenomena in steels. In the early days, models assuming local equilibrium at the phase boundary were used. An example of such a model is the Johnson–Mehl–Avrami–Kolmogorov (JMAK) approach, commonly referred to as the Avrami model, which is widely used to simulate phase transformations due to its simplicity and analytical nature (Shirzad & Viney, 2023). JMAK-based models describe the kinetics of phase change by assuming uniform nucleation and isotropic growth of new phases within a homogeneously transforming material. The transformation fraction as a function of time is expressed through an exponential relationship involving parameters related to nucleation rate, growth rate, and dimensionality of the transformation. These models belong to the phenomenological class of methods and thus do not account for local microstructural heterogeneities or spatial interactions between grains. However, they still provide valuable insights into the overall transformation behavior, particularly for isothermal processes. They are often used in combination with experimental data to extract transformation kinetic parameters and serve as a benchmark for more complex, spatially resolved models. Over time, approaches that are not based solely on analytical methods have been developed, integrating, among other things, the limited mobility of the phase boundary, diffusion resistance and the influence of previous plastic deformation. These models, belonging to the mean-field or full-field class, can incorporate critical microstructural heterogeneities, complex thermodynamic databases and kinetic parameters derived from experimental data or CALPHAD (Calculation of Phase Diagrams) assessments (Spencer, 2008), allowing for realistic predictions of phase distribution, grain morphology, and transformation kinetics under varying processing conditions (Deffrennes et al., 2023).

Modern numerical methods, for example Phase-Field (PF), Level-Set (LS), Cellular Automata (CA), or Monte Carlo (MC) methods, enable the detailed simulation of microstructure evolution and phase transformations under various technological conditions (Gomez et al., 2019; Szeliga et al., 2020). Furthermore, the recent coupling of these models with machine learning techniques is opening new possibilities for data-driven optimization of steel design and processing (Cheloee Darabi et al., 2023). This synergy between experimental observation and theoretical modeling forms the cornerstone of modern computational materials science and advanced materials engineering.

This work focuses on the analysis of the state of the art in the area of numerical methods for modeling the γ → α transformation in steels. Particular attention has been paid to the use of a hybrid approach based on cellular automata and the finite difference method (FDM), which allows for the efficient representation of diffusion processes and ferrite grain growth during cooling. The purpose of this paper is to present the advantages and limitations of various methods and to outline directions for their further development in an industrial context.

2. Full-field methods

Phase transformations in steels and alloys involve changes in microstructures, such as the formation of new phases (e.g., ferrite, martensite) or the precipitation of particles, which significantly affect material properties. As mentioned, full-field modeling approaches explicitly simulate the spatial distribution and evolution of phases within a material, unlike mean-field models, which only use averaged information (Szeliga et al., 2020). A variety of approaches have been developed over the years, and the most commonly used are evaluated in the following sections. Each of the investigated methods has unique principles, advantages, and limitations, making them suitable for different length scales and types of transformation phenomena (Gomez et al., 2019; Madej et al., 2016).

2.1. Phase-Field method

The PF method employs a diffuse-interface approach, meaning it represents interfaces between phases as smooth gradients rather than sharp boundaries (Fig. 1). This is achieved through the use of continuous field variables known as order parameters (Tourret et al., 2022). These parameters indicate the presence of distinct phases within the material in particular areas. In multi-phase systems, multiple order parameters may be necessary to capture the characteristics of each phase. The evolution of these order parameters and other field variables, such as composition, is governed by partial differential equations (PDEs) derived from thermodynamic principles. Two key types of equations are used in this method: the Allen–Cahn equation for non-conserved order parameters (Chen L.-Q. & Zhao, 2022), which governs interface motion without conserving the volume of each phase; and the Cahn–Hilliard equation for conserved fields (Wu, 2022), which describes the diffusive redistribution of solute. These equations ensure that the simulation adheres to thermodynamic driving forces and kinetic laws (Yamanaka, 2023).

A significant advantage of the PF method is its efficiency in modeling the evolution of complex microstructures (Chen L.-Q., 2002; Moelans et al., 2008). Instead of requiring explicit front-tracking algorithms to monitor every interface, the method allows interfaces to emerge naturally as narrow transition regions where order parameters change values (Fig. 2). Such a concept is often classified as a front-capturing approach (Chen L.-Q., 2002). This concept simplifies the computational process while maintaining physical realism. Its versatility is evident in its ability to simulate complex morphologies, such as lamellae, without the need for manual interface tracking, thereby enhancing computational efficiency and reducing errors. Moreover, this method's foundation in thermodynamic consistency allows it to seamlessly integrate with free-energy frameworks and databases like CALPHAD, ensuring accurate modeling of phase diagrams and thermodynamic data in multicomponent systems (Liu C. et al., 2021). Furthermore, the PF method is capable of accommodating various physical effects such as solute diffusion, elastic strains, plasticity, electromagnetic fields, and thermal fields through additional terms or equations. This capability is particularly demonstrated in modeling martensitic transformations (Mamivand et al., 2013), where elasticity coupling helps describe lattice distortions, thereby showcasing its broad applicability across various material systems. In addition, its adaptability extends to the modeling of a wide range of phenomena, including solidification, solid-state transformations in steels, precipitation and dissolution processes (Hallberg, 2011; Kobayashi, 1993; Thiessen et al., 2007; Xu & Meakin, 2008).

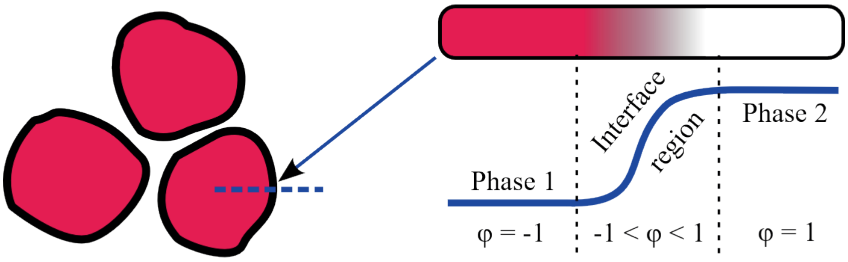

Fig. 1. Description of the interfacial boundary using the phase-field method

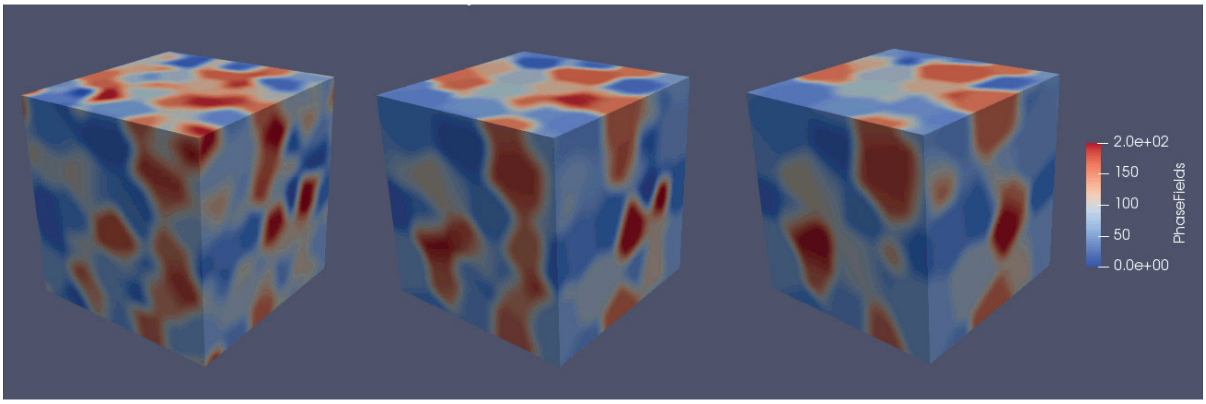

Fig. 2. Simulation of grain growth and nucleation by the Phase-field method in subsequent steps

As described, the PF method is a powerful tool for studying microstructural evolution but faces challenges related to computational demands and practical implementation. The most common problem is computational intensity due to the need for the fine grid resolution of the diffuse interface (Zhang Jin et al., 2023). Mesh spacing is supposed to be smaller than the interface width to accurately resolve these diffuse interfaces. This results in large numbers of integration points, especially in 3D simulations, and can be particularly time-consuming when combined with small time steps required for solution stability and accuracy. While adaptive mesh refinement can help concentrate appropriate finite element resolution at interfaces, it adds complexity and overheads. As a result, phase-field methods are more computationally demanding than alternative techniques such as CA or MC. At the same time, the diffuse-interface approach involves solving coupled PDEs across the entire domain at each time step, which poses challenges for parallelization. Although many open-source phase-field codes support high-performance computing (HPC), the parallel efficiency is often lower compared to discrete methods like MC simulations, as phase-field requires global communication of field variables and implicit equation solving (Chafia et al., 2024; Ghosh et al., 2022; Hu et al., 2024). Model parameter calibration is another critical issue (Qin & Bhadeshia, 2010). To achieve quantitative results, interface parameters such as width and mobility must be related to physical values. If the selected interface thickness is artificially large for computational efficiency, corrections or asymptotic analysis are necessary to ensure the accurate reproduction of sharp-interface kinetics, thereby avoiding so-called “thin interface” artefacts. Therefore, determining kinetic parameters (e.g., interface mobility, nucleation conditions) that align with real material behavior remains a challenge. The handling of nucleation poses additional difficulties (Hu et al., 2024). In classical phase-field models, new phase regions are introduced either through the imposition of initial nuclei or fluctuations induced by the addition of noise. However, capturing heterogeneous nucleation at specific sites (e.g., grain boundaries or inclusions) is not straightforward and often requires ad hoc approaches, such as introducing nuclei based on probability or employing specialized free energy terms (Mecozzi et al., 2008; Schoof et al., 2018).

2.2. Level-Set method

The LS method is another computational technique that is often used to model moving interfaces in the microstructure. In this case, the interfaces are represented implicitly using a higher-dimensional function, typically denoted as $\varphi(x, y, z, t)$, which depends on coordinates x, y, z and time t. This function acts as a signed distance field, where the interface corresponds to the contour (Fig. 3) of a particular feature. Instead of tracking the interface directly with markers or mesh points, the LS method updates this function over time according to a PDE. This implicit formulation allows for the efficient handling of topological changes without the need for complex marker management (Osher & Sethian, 1988).

The LS method offers a precise geometric representation of interfaces through an implicit approach, eliminating the need for parametric tracking. It maintains sharp interfaces and provides geometrical properties, such as normal to grain boundaries and their curvature, via the differentiation of the LS field (Bernacki, 2024a; Ervik et al., 2014; Lervåg & Ervik, 2013). This formulation naturally handles topological changes as φ evolves, accommodating complex interface dynamics without requiring special implementation of the additional solutions. An additional benefit of LS is its straightforward extensibility to three dimensions (Fig. 4), allowing it to be compatible with finite difference or finite element methods. It avoids challenges like mesh tangling associated with explicit front-tracking. It has proven effective across various application fields, including fluid dynamics (Ning et al., 2023) and image processing (Osher & Tsai, 2003), and particularly for the mentioned curvature-driven grain growth (Zhang X. et al., 2008). LS couples well with continuum field calculations, such as heat flow or diffusion, due to the coupling possibility with discretized space. This allows simultaneous solution of diffusion or thermal equations on the same grid, enabling modeling of transformations influenced by field variables. It is worth mentioning the LS method exhibits higher computational efficiency compared to PF formulations, especially in diffusive phase transformations (Jacobsson et al., 2024). This is because only the interface region requires fine resolution, while bulk regions are computed with coarser resolution. As a result, LS may utilize fewer degrees of freedom or allows for the application of larger time steps.

The classical LS method works well for describing a two-phase system, i.e., one phase boundary. However, a large number of level-set functions are required, or an extended implementation of regions is needed when dealing with many grains or phases. For example, in modeling grain growth, each grain can be assigned its own level-set function, or they can be combined iteratively in pairs. With a larger number of grains, this becomes increasingly complex and computationally demanding, requiring dedicated solutions like level-set function re-initialization solutions (Murgas et al., 2022; Zhang X. et al., 2008).

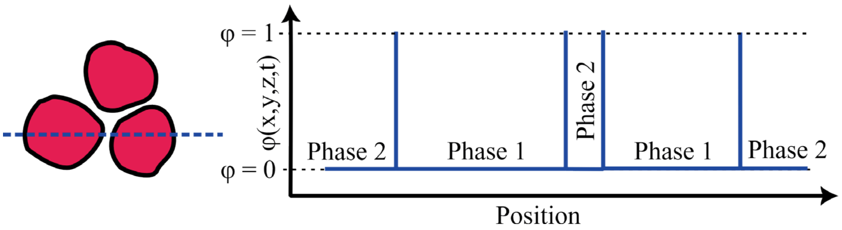

Fig. 3. Diagram of the level-set method showing the cross-section of the computational domain as a φ function

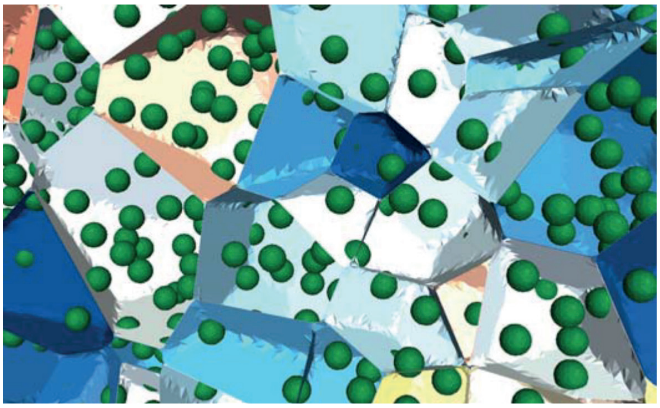

Fig. 4. Three-dimensional LS microstructure for Inconel 718 alloy with second phase particles (green spheres) from the work by Scholtes et al. (2016)

Managing multiple boundaries and their mutual interactions is more challenging compared to the PF method, where multiple ordinal parameters can be used simultaneously. This affects the applicability of the level-set method in highly complex multi-phase structures. However, there are strategies for handling this, such as assigning each grain its own function or using coloring algorithms. To ensure that the function φ maintains the property of a distance function, it needs to be reconstructed periodically. This reconstruction involves additional computational costs. Furthermore, to reduce these costs, a so-called "narrow band" (Fig. 5) is often used (Olshanskii et al., 2024; Osher & Fedkiw, 2001). This means that function φ is only updated near the phase boundary, which increases the complexity of the implementation.

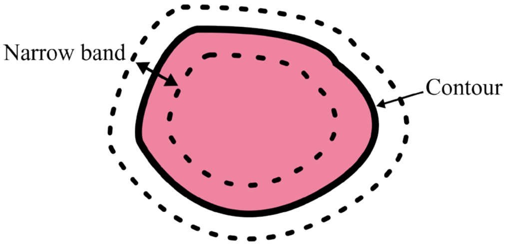

Fig. 5. Narrow band method for optimizing computation time in the level-set method by limiting the computation area

Although the phase boundary is theoretically sharp, its precise numerical representation requires an appropriately fine grid, which is somehow similar to the PF approach. A mesh of great precision must describe small feature curvatures or thin, layered structures. During diffusive transitions, the thickness of the phase boundary often spans only a few grid cells, resulting in sharp concentration gradients. To accurately represent and preserve continuity, a mesh as detailed as that used in the phase-field method is needed. Often, an adaptive mesh is employed near the boundary, which increases computational cost. The LS method does not naturally describe nucleation processes or crystallographic texture (Mourad & Garikipati, 2006). New phase boundaries must be introduced arbitrarily based on predefined criteria. Therefore, this method does not account for the spontaneous formation of new phases or their crystallographic orientations. Suppose crystallographic orientation plays a crucial role, like in anisotropic growth or martensitic transformations. In these cases, the LS does not capture changes in orientation but describes only the geometry of the boundary. It also struggles with handling texture evolution under large plastic deformation. To incorporate such effects, coupling with other models or methods is required, such as CA (Szeliga et al., 2020) or FEM (Bernacki, 2024b). The application of them enables the LS method to use and provide information about the interior regions of grains, enhancing its capabilities. However, the hybrid approach increases the complexity of the model and, therefore, may impose limits on the use of space and increase calculation time (Khedkar et al., 2025).

2.3. Cellular Automata method

The CA method is one of the discrete methods in which the computational space (automaton) consists of CA cells with regular shapes, usually providing a regular simulation grid (Sarkar, 2000). Each CA cell represents a small volume of material with a defined state. The primary state evolution mechanism of this method involves updating the state of each CA cell in successive time steps according to predefined transition rules. These rules utilize information stored in the considered CA cell, as well as from its local neighborhood. Transition rules are used to capture the physics behind the investigated phenomena, such as recrystallisation, phase transformations or grain growth. A key feature of cellular automata is the concept of neighborhood, which refers to a set of adjacent cells. In a 2D space, eight surrounding cells form the Moore neighborhood, while four form a von Neumann neighborhood (Fig. 6).

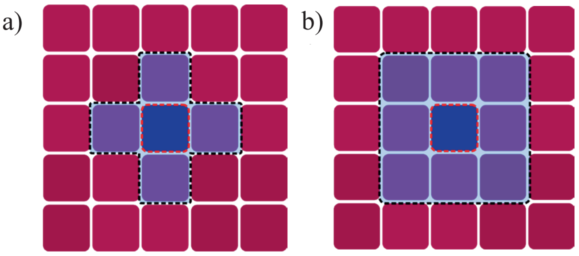

Fig. 6. Neighborhood diagram: a) von Neumann; b) Moore for 2D automata with cubic cells

The transition rules analyze both the neighboring CA cell configuration and the current cell's state to determine its new state (Fig. 7). The update of CA cell states can occur synchronously (all CA cells at the same time) or asynchronously (Schönfisch & de Roos, 1999). In many microstructure models, a synchronous approach is employed, where all cells evaluate their neighbors' states from the previous time step before updating their own states simultaneously. Time in CA simulations progresses in a discrete manner, which can be calibrated to correspond to real physical time (Wolfram, 1984).

Using the CA method does not require solving complex differential equations; instead, it uses logical rules and possible random number inputs for probabilistic events. Each cell interacts only with its nearest neighbors, giving the algorithms a local character. Due to this and the separation of calculating the new state stage from applying these changes, this method is well-suited for parallel computing (Hansen, 1993). CA algorithms can be efficiently parallelized across multiple processors or computing nodes with minimal communication overhead. This makes CA especially effective for large-scale simulations of phase transformations in steels, where high spatial resolution is necessary to accurately capture grain nucleation, growth, and impingement (Sitko & Madej, 2016). It's worth mentioning that CA effectively represents the inhomogeneity of microstructures. This enables the realistic modeling of differences in grain size, shape, and distribution of element concentration, as well as dislocations or stored energy. Additionally, while cellular automata models operate discretely, they can be combined with continuous calculations, such as finite element simulation of temperature distribution. Often, they are also combined with other numerical methods, e.g., finite differences (FD) (Opara & Kuziak, 2020) or finite element (FE) (Gawąd et al., 2008). The FD or FE solver calculates the field of temperature or diffusion, and cellular automata use this data to determine when a phase change occurs. For example, in solidification modeling, the temperature curve for each cell is provided by the temperature solver (Zyska et al., 2018). When it drops below the liquidus line, the cell changes state from liquid to solid according to the dendrite growth rules. This combination brings together the strengths of CA for detailed microstructure description with the precision of continuum theories in describing physics (Opara & Kuziak, 2020; Sitko & Madej, 2021; Zhi et al., 2024).

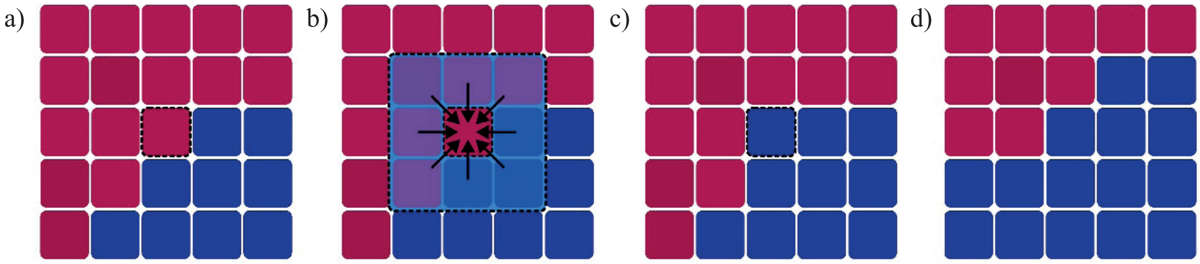

Fig. 7. The stages of the CA method: a) considering the state of the CA cell and internal parameters; b) collecting information from neighboring cells; c) determining the new CA cell state. In the case of d), the space is presented in a final form after considering all CA cells in a given time step

At the same time, the CA method has several significant limitations. One of them is the dependence of results on the geometry of the grid, that is, the influence of artificial anisotropy (Shi et al., 2022; Wei et al., 2016; Wermiński et al., 2025). Growth directions align with grid axes, potentially leading to unnatural effects such as deformed growth fronts if rules are not carefully chosen (Fig. 8). To mitigate this effect, strategies include expanding neighborhoods, randomizing growth directions, or using hexagonal grids have been developed (Marek, 2013). The CA's discrete nature makes models also less precise for curvature and phenomena like the Gibbs–Thomas effect compared to continuous methods (Liang X. et al., 2023).

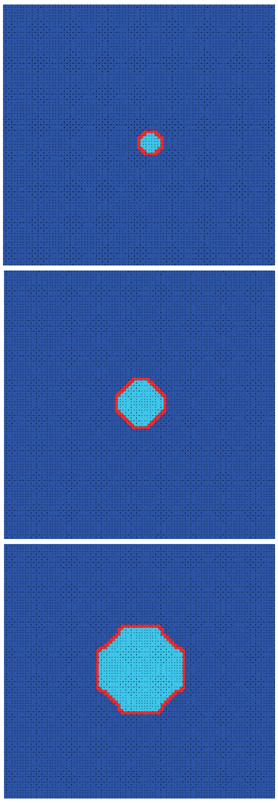

Fig. 8. Grain geometry during growth in successive steps of phase transformation simulation with visible influence of CA space on the final shape of the grain

As mentioned, in the CA, each CA cell represents a volume element, so boundaries are at the cell level, requiring fine grids or numerical smoothing for smooth, curved interfaces. Another problem is that CA rules lack assigned physical units, necessitating calibration of time steps and CA cell sizes to match real-world scales (Ghumman et al., 2023). This calibration can constrain the model's predictive capabilities beyond its adjusted range. Continuous and randomized methods, such as the MC or PF approaches, describe curvature more directly in terms of energy, offering better accuracy for physical effects like surface tension. Thus, while CA is effective for large-scale structures, it has limitations in handling small details and certain physical aspects.

2.4. Monte Carlo method

The classical Monte Carlo (MC) method, such as the Metropolis algorithm, involves random sampling of system states according to a probability distribution dependent on energy. In materials science, it is often employed in conjunction with lattice models, such as the Potts model, for simulating microstructures (Wright et al., 1997). For instance, individual MC cells in the MC space are assigned states corresponding to different phases or crystallographic orientations, and state changes are accepted with a specific probability to reflect the system's tendency to minimize energy, such as interfacial energy (Fig. 9). This method allows for the study of system evolution toward equilibrium or metastable configurations with an element of thermal fluctuation. In grain growth, it mostly causes small grains to disappear and larger ones to grow (reducing boundary energy). For phase separation or ordering, it can also simulate domain coarsening (Sitko & Madej, 2016). However, unlike CA, which follows deterministic kinetic rules, the Monte Carlo approach follows a thermodynamic driving force through probabilistic changes.

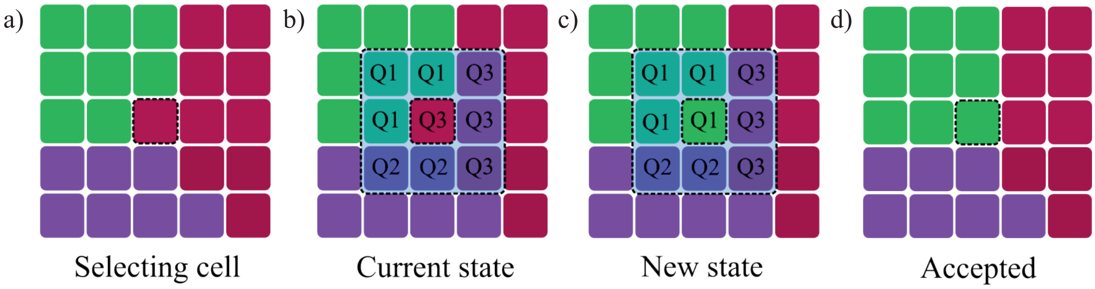

Fig. 9. The stages of the MC method: a) selecting a random cell in the MC space; b) calculation of energy based on the current MC cell state and the states of neighboring cells; c) calculation of energy after new state assignment; d) accepting a new state with a certain probability calculated using the difference in energy before and after the change

Similar to cellular automata, Monte Carlo simulations can be conducted on large 2D or 3D lattices. It can also be done by applying parallel algorithms (Preis et al., 2009). However, this method is asynchronous, so care must be taken to avoid read-write conflicts (Weigel, 2017). Various strategies exist to address this issue. It should be mentioned that MC has a physical basis related to feature curvature. The approach based on energy naturally incorporates the tendency to minimize the surface area of boundaries. It can be shown that, in the limit of a large system and low "temperature," the Potts model yields kinetics consistent with grain growth driven by curvature. This establishes a semi-quantitative connection with the physics of surface structure evolution. While the basic Potts model minimizes only boundary energy, it can be extended by adding additional terms to the energy function. For example, a term can be added that gives certain orientations an energetic advantage – this represents stored energy due to deformation. Additionally, interaction energy can be introduced to facilitate neighbor relationships for specific phases, aiding in simulations of dislocations or phase ordering.

The main drawback of the Monte Carlo method is that it does not have a direct connection between MC steps and real-time (Wermiński et al., 2023). To compare MC simulation time with physical time, adjusting the MC steps relative to the experiment or another model is necessary. There are different approaches – for example, matching the growth rate to a known flow curvature equation or reflecting through values of grain boundary mobility. However, there is no clear, direct relationship by default. This means that MC effectively exhibits qualitative behavior and normalized kinetics, but precise time prediction requires additional assumptions (Raabe, 2000). Another issue is that the lattice in the Potts model enforces the discretization of position boundaries between grains. Boundaries "tremble" and shift by lattice units. On a large scale, this works correctly; however, it may introduce slight anisotropy, as boundaries prefer to move along specific lattice directions (Mason et al., 2015). This can be mitigated by using a large number of possible states and smoothing algorithms. It is also worth mentioning that the standard Potts model does not solve equations of diffusion or stress equilibrium. It only aims to reduce boundary energy by a probabilistic rule. Therefore, when changes occur that involve long-range diffusion (e.g., the growth of new phases with composition changes), the Potts model alone is insufficient. Similarly, it does not represent elastic deformation energy unless added to the energy functional. Some researchers incorporate components that penalize configurations causing deformation (Williamson & Delplanque, 2015). However, this significantly complicates the MC model. A notable feature of this method is that, due to the stochastic nature of MC, the results contain unavoidable noise. Typically, many runs are performed, and data is averaged, or a large system is simulated to achieve smooth and representative behavior. Key events, such as nucleation, may require multiple trials to obtain statistically significant results. If the model parameters are not set properly, the results may be far from the physics; for example, feature boundaries can become unnaturally rough or the system becomes stagnant (pinning effect). Therefore, the MC model parameter must be carefully adjusted to suit the specific problem, which is not an easy task.

2.5. Vertex method

The vertex-based model describes the microstructure of polycrystals by directly representing the geometry of grain boundaries. In a 2D case, grains are represented as polygons, with their edges being line segments connecting vertices where three grains meet at triple points. In the 3D case, grains are polyhedrons with flat faces that meet along edges and vertices. The fundamental concept involves tracking the movement of these vertices, along with their corresponding grain boundary edges, according to physical laws such as curvature flow and energy minimization. In the typical 2D model of grain growth, the position of each vertex is updated by solving its equation of motion. This equation arises from the equilibrium of the grain boundary tensions at that vertex where three grains meet. The velocity of an edge's movement is often proportional to its curvature and mobility (Fig. 10). The vertex-based model essentially solves these equations for all vertices simultaneously. As a result, the grain structure changes: edges move, part of them shrink, and others disappear (Fuchizaki & Kawasaki, 1995; Kawasaki et al., 1989; Lépinoux et al., 2010; Syha & Weygand, 2010).

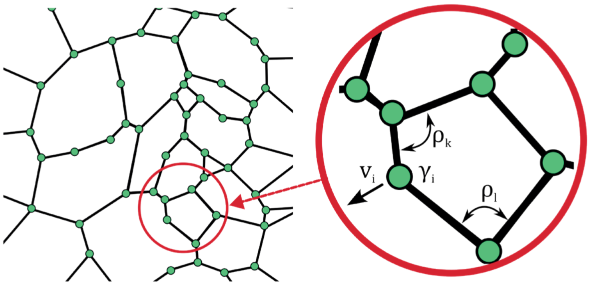

Fig. 10. In vertex method simulations, a velocity v is calculated for each vertex based on the assigned grain boundary energy γ and mobility. Information on angles ρ between grain-forming segments is often used to ensure equilibrium at grain junction points

The model based on this method can represent grain boundary lines as continuous smooth curves or straight-line segments between vertices. They are not confined to a pixel grid, allowing for precise representation of curvature and length within the set resolution of vertices. This facilitates accurate modeling of processes dependent on curvature, such as grain growth. In this case, the number of degrees of freedom increases proportionally to the number of grains (vertices), rather than the total area or volume. This makes it efficient for simulations with a moderate number of grains, especially when there are a few hundred grains. Another important feature of this approach is the possibility to incorporate the anisotropy (Enomoto et al., 1996; Hallberg, 2011). The vertex model can easily account for the anisotropic properties of grain boundaries. These properties vary depending on the angle between crystals or the orientation of the boundary plane. Equilibrium at the vertices can reflect these differences, enabling phenomena such as abnormal grain growth, where some boundaries move faster or slower depending on their angles.

On the other hand, vertex-based models have primarily been developed for describing grain growth in single-phase microstructures. Their application to phase transformations (where a new phase nucleates and grows) is more challenging. Nucleation of a new phase means introducing a new closed boundary loop into the lattice. The method is capable of doing so, but the user has to specify when and where to add new vertices and edges (Hallberg, 2011). Furthermore, the method is not well-suited for cases where simulating a large number of grains. If the grains become very small compared to their neighbors, algorithms in this method can randomly remove them to prevent them from being reversed or distorted. Compared to grid-based methods, this method is much more complex. The reason is that geometry and topology must be handled carefully, i.e., detecting events, determining how to restructure the lattice, managing the addition and removal of vertices, and ensuring the numerical stability of vertex movements (Torres et al., 2015). These limitations introduce practical limits on the number of grains and their size. It is worth emphasizing that vertex-based models primarily focus on boundary motion driven by curvature and surface energy. They do not account for diffusion in the bulk or the thermodynamics driving transformations. Therefore, these models are best suited for phenomena driven by capillarity, such as grain growth within one phase.

2.6. Comparison of Full-Field methods

As presented, full-field methods, such as phase-field, level-set, cellular automata, Monte Carlo, and vertex, are widely used to model phenomena in materials. Each of these methods has its strengths but also its limitations, which are summarized in Table 1.

The phase-field method enables the accurate representation of shapes and the evolution of phase boundaries. However, it is computationally very expensive. The level-set method also effectively describes moving interfaces. However, it requires advanced numerical techniques and can have problems with mass conservation. Cellular automata are simpler and faster to implement than the PF and LS. They are suitable for large-scale simulations but are sensitive to artificial anisotropy. Monte Carlo simulations effectively reproduce statistical processes, such as recrystallisation. However, it does not always provide physical realism. The vertex method, on the other hand, properly captures the topology and migration of boundaries in polycrystal structures but its applicability to multiphase or 3D systems is limited. The choice of method depends on the phenomenon being studied, the required accuracy, and the availability of computational resources.

Table 1. Comparison of evaluated full-field methods with respect to their capabilities in microstructure evolution modeling

Method	Key features	Advantages	Limitations
Phase-Field (PF)	diffuse interface, thermodynamically consistent PDEs	handles complex morphologies, elastic/plastic coupling	high computational cost, needs a fine mesh, difficult nucleation modeling
Level-Set (LS)	sharp interface via signed distance function, implicit boundary tracking	efficient for tracking sharp interfaces, natural topological changes	complex for multi-phase/multi-grain systems, requires periodic reinitialization
Cellular Automata (CA)	discrete grid, sharp interface, transition rule-based system evolution with neighborhood role	efficient, suitable for parallelization, handles large-scale structures	grid-induced anisotropy, lacks physical units, lower accuracy in curvature
Monte Carlo (MC)	discrete grid, sharp interface, probabilistic state change based on energy minimization	captures thermodynamic tendencies, curvature-driven grain growth	no natural time scale, discretization artifacts, high noise level
Vertex	tracks grain boundary vertices, geometric and topological updates	precise boundary representation, supports anisotropy in curvature-driven growth	limited to grain growth, complex implementation for topology changes

This work specifically addresses phase transformation modeling; therefore, the state of the art in this area is further expanded in the following chapters.

3. Modeling γ → α phase transformation in Fe-C and Fe-C-M systems

Modeling phase transformations in steels during cooling has undergone significant theoretical evolution in recent decades (Bhadeshia, 2010; Gamsjäger et al., 2006; Gaude-Fugarolas & Bhadeshia, 2003; Gomez et al., 2019; Gouné et al., 2015; Hackenberg, 2012; Hillert, 1999). With particular emphasis on the transformation of austenite into ferrite, early research was dominated by an approach assuming local equilibrium at the phase boundary, specifically, the Local Equilibrium (LE) model (Bhadeshia, 2021). Classical frameworks were based on describing the growth of ferrite nuclei as a phenomenon controlled solely by diffusion, with the assumption that the transformation occurs in accordance with thermodynamic equilibrium between phases. The turning point in the development of models was introduced in the article by Van der Ven & Delaey (1996) where the formalism of irreversible thermodynamics was applied to analyze the iron potential during isothermal transformations in Fe-C and Fe-C-M systems. In this model, the γ/α boundary was considered a surface with infinite mobility, and the kinetics of the transformation were determined by carbon diffusion in the austenite. The authors indicated that the dissipation of free energy during transformation could result from various processes: volume diffusion, interface migration, or solute drag effects. They introduced an analysis of different kinetic regimes, describing transformations not only as diffusion-controlled but also influenced by interfacial properties such as their resistance, structure, and mobility.

This approach was further developed in models considering out-of-equilibrium conditions at the phase boundary, as in the work by Krielaart et al. (1997). The authors introduced a numerical model where the actual mobility of the interface is finite, and local equilibrium conditions are not satisfied. In this framework, interface migration depends not only on the chemical potential difference between phases but also on the local carbon concentrations on both sides of the phase boundary. This approach yields a description of transformations in a mixed mode (Fig. 11). Consequently, this model accounts for the transition from a diffusive transformation at low undercooling to an interface-controlled transformation at higher undercoolings.

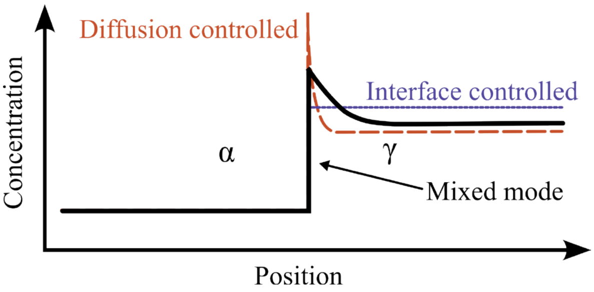

Fig. 11. Carbon concentration profile at the interface for growing ferrite grain in austenite matrix. Variants of the control of diffusion and mobility of the interface present two extremes, in which, respectively, diffusion is low, and mobility is infinitely high, and conversely

The issues of solute drag and trapping in out-of-equilibrium conditions were explored in depth by Hillert (1999). In his comprehensive review, he presented a comparison between approaches based on Gibbs energy dissipation and classical sharp-interface and diffuse-interface models (Fig. 12). He pointed out that at high interface migration velocities, phenomena occur that cannot be captured by models relying on local equilibrium assumptions. Specifically, interface acceleration can lead to the accumulation of alloying elements at the phase boundary and a reduction in the driving force for transformation. Parallel development was carried out for kinetic models incorporating the interaction between diffusion and interface motion. In an article by Svoboda et al. (2001), a boundary condition was proposed based on the kinetics of phase boundary migration, taking into account both chemical and mechanical contributions to the driving force of transformation. This enabled the model to predict composition changes and microstructural evolution, even in the presence of stresses arising from phase lattice mismatch.

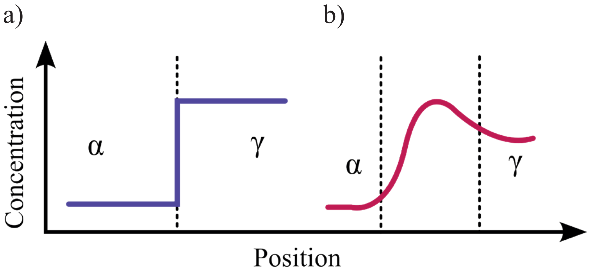

Fig. 12. Sharp (a) and diffusive model (b) of the interface with marked area of the phase boundary

In the context of technological applications, research on the γ → α transformation under real hot rolling and cooling conditions holds significant importance. Leeuwen et al. (2003) demonstrated that this transformation can occur in a mixed mode, with its nature potentially evolving during the process based on local concentration and geometrical conditions. By employing carbon concentration analysis at the γ/α boundary, the authors demonstrated the feasibility of quantitatively determining the transformation's character, ranging from interface-controlled (when the local concentration approximates average levels) to diffusion-controlled (as it approaches equilibrium values). Sietsma & Zwaag (2004) formally generalized these assumptions by proposing a single-parameter model based on the Z factor, which is a function of diffusion, interface mobility, and the geometry of the growing phase. This parameter enables a clear determination of the transformation's nature at any point during its process. A significant conclusion from their work was that every transformation begins as interface-controlled; however, as the new phase grows, it progressively shifts to being diffusion-controlled. Experimental confirmation of these concepts was provided by Liu Y. et al. (2006), who analyzed the effect of cooling rate on the shape of transformation kinetics. It was found that at low rates, the transformation occurs in a diffusive mode; however, at high cooling rates, it exhibits a massive character driven by interface mobility. Similar conclusions were presented in article by Chen H. et al. (2010). Here, a modified JMAK model incorporating sequences of transitions between different growth modes from interfacial through diffusive to re-interfacial was used. An important supplement to kinetic models considers the influence of prior plastic deformation of austenite on the driving force and transformation kinetics. Sietsma (2012) noted that the presence of defects arising from plastic deformation, such as dislocations or grain boundary distortions, significantly lowers the energy barrier for ferrite nucleation, thereby increasing the density of nuclei and accelerating the entire transformation process.

In the work of Chen H. & Zwaag (2014), a new modeling framework called the Gibbs Energy Balance (GEB) model was introduced as a generalization of the mixed-mode approach for multicomponent Fe-C-M alloys. This model incorporates a physically and thermodynamically consistent treatment of substitutional alloying element M diffusion (such as Mn and Ni) within the migrating interface. It bridges the gap between classical local equilibrium (LE) and paraequilibrium (PE) conditions, demonstrating that both can be derived as limiting cases of a more general formulation. A novel feature of the GEB model was its capacity to predict "transformation stasis" – a state in which the phase transformation slows down/stops due to an insufficient chemical driving force to overcome the combined dissipation from solute drag and interface friction. This was demonstrated experimentally and modeled for Fe-C-Mn and Fe-C-Ni alloys, showing that elements like Mn significantly intensify the stasis effect due to their high partitioning coefficients and interaction energies.

The presented models are widely used in full-field modeling. They are treated as concepts that are implemented using methods like PF, CA, MC or Vertex method. They help to understand how certain phenomena work during transformation, and they can be used as a tool for validation and parameters identification. The following sections discuss the application of the various full-field methods to model the austenite-ferrite transformation based on the considerations outlined above.

3.1. Phase-field models of austenite-to-ferrite Phase Transformations

Pariser et al. (2001) presented the first simplified model to simulate the γ-α transformation in ultra-low-carbon (ULC) and interstitial-free (IF) steel grades. In this work, the model highlighted the critical role of nucleation undercooling and interface mobility parameters. Although showing promising agreement with experimental results, it also emphasized the need for further improvements in model parameter identification. Then, Loginova et al. (2003) discussed the transition between diffusion-controlled and massive transformation γ → α in binary Fe-C alloys. This work combined the solute drag effect with a 1D phase-field approach and thermodynamic models, where the space was limited to the boundary of only one grain. In a subsequent paper (Loginova et al., 2004), the authors introduced an extension of a previous approach to a 2D model, allowing for the analysis of Widmanstätten ferrite plate formation from an austenite grain boundary. This model uniquely captured different growth morphologies (diffusion-controlled, Widmanstätten, and massive) within a single phase-field formulation, significantly extending the capabilities of previous models. Another 2D model was presented in (Mecozzi et al., 2005), where the PF approach was used to examine the effects of interface mobility and niobium carbide precipitation on the kinetics of ferrite formation during controlled cooling from different austenitisation temperatures. The primary limitation of this work was the dependence on the fitted parameters of the model. The interfacial mobility was not measured independently but was adjusted to achieve an optimal fit to experimental data, which negatively impacted the predictive capabilities of the model. Another solution introduced in (Huang et al., 2006) was capable of simulating γ-α transformation kinetics in low-carbon steels over large spatial and temporal domains during both isothermal and continuous cooling transformations. As before, there was a problem with the need to adjust model parameters, and it showed limitations in predictive capabilities at high cooling rates due to simplified nucleation assumptions. Although this model successfully simulated interface movement, considering grain impingement and solute enrichment. Moreover, a modified version of this model was presented in the article by Huang et al. (2006), considering the grain coarsening mechanism.

At the same time, Militzer et al. (2006) demonstrated the extent to which results can differ when the PF are conducted not in 2D but in 3D space. The authors demonstrated that the transformation rates observed in 2D are noticeably faster than those in the 3D case, resulting in underestimated mobility values when compared with experimental data. Additionally, the morphology of the remaining austenite toward the end of the simulation was more accurately captured in 3D, whereas in 2D it often appeared unrealistic. As a result, three-dimensional simulations yield far more accurate representations of the final non-ferritic transformation products, such as pearlite, bainite, and martensite. In the article by Mecozzi et al. (2008), the authors used a 3D model to analyze the interplay between the nucleation temperature range and effective interface mobility and validated the results against the experimentally obtained transformation kinetics. They demonstrated that broader nucleation temperature intervals require higher interface mobility to match experimental data.

Several studies in the literature have also focused on extending 2D models to 3D space by incorporating additional modules. The model presented in the publication by Suwanpinij et al. (2009) integrated experimentally observed nucleation behavior and deformation-induced changes in driving force to simulate microstructural evolution during isothermal holding. Another work (Cha et al., 2010) introduced a model, that explicitly incorporated the elastic lattice effects caused by the volume mismatch between the two phases in a binary Fe-C system. The authors build on earlier phase-field and elasticity models, combining them to predict the nucleation, growth, and morphological evolution of ferrite under different cooling rates, grain sizes, and wetting angles.

However, in recent years, the direction of research shifted onto the pearlitic, bainitic and martensite transformations (Yamanaka, 2023). According to the austenite-pearlite transformation, Mushongera et al. (2018) introduced a complex model to study the formation and development of divergent pearlite structures in ternary Fe-C-Mn steels in isothermal conditions. The authors presented a detailed analysis of how local changes in elemental composition and cooling conditions affect the initiation and propagation of pearlite branching, which could not be observed with binary approaches. In further work (Mushongera et al., 2020), the model was extended to use partitioning local equilibrium conditions at the interface. The authors argue that in Fe-C-Mn systems, the assumption of classical local equilibrium known from binary systems cannot be applied. In addition, particular attention was paid to the role of manganese diffusion, demonstrating that its low mobility and strong reduction of phase boundary energy have a key influence on the rate and direction of new phase development. Another interesting work is the article by Wang K. et al. (2025), which focuses on multiphase modeling of the transformation of austenite to pearlite and ferrite in hypoeutectoid steels. The model takes into account the influence of cooling rate, primary austenite grain size, and carbon content on the amount and morphology of pearlite and on the microstructure of ferrite, providing a complete quantitative analysis of these relationships.

3.2. Level-set models of austenite-to-ferrite Phase Transformations

The level-set method was first applied to model diffusive phase transformations in steels in the work by Iwamoto et al. (2008). Iwamoto and his team introduced a model based on the finite element method and level-set approach. This enabled the simulation of phase boundary movements driven by diffusion during cooling. In their study, they demonstrated that the LS method effectively models complex shapes of interphase boundaries during solid-solid phase transformations. It laid the foundation for further research, demonstrating that the LS method enables the natural reproduction of phenomena such as merging, splitting, and any movement of phase boundaries.

Then, Barbe & Quey (2011) developed a fully three-dimensional LS model for simulation of the diffusive austenite-to-ferrite transformation at the polycrystalline scale. Their work is notable because it incorporated crystalline plasticity into the phase transformation model. Moreover, this model enabled the tracking of the evolution of three-dimensional phase boundaries using the LS function. The work represented a significant advancement from earlier models, which typically considered only one phase boundary or one grain. This allowed to explore how mechanical deformations and phase transformations mutually influence each other. Furthermore, it demonstrated how stress and plastic deformation in austenite influence the growth of ferrite grains, providing a more realistic simulation of microstructure development in two-phase steels.

At the same time, the work by Hallberg et al. (2010) explored the application of LS methods in the thermomechanical context. The authors developed a model for martensitic transformation in steel that included thermomechanical coupling. The proposed approach was based on internal variables rather than directly on the LS method.

For the following years, the high computational cost of 3D LS simulations remained a challenge. Strategies based on representative volume elements were then applied to reduce the system complexity. In the article by Bzowski et al. (2021) a comprehensive model of the microstructure development in bainitic steel during intercritical heating was developed, where interface tracking from the LS method was combined with the so-called statistically representative volume element (SSRVE) concept. This allowed for a reduction in the size of the computational domain required for simulation, opening the way for more extensive analysis at industrially relevant scales. In this model, the phase boundaries between austenite and ferrite were tracked using cross-sectional functions, while carbon diffusion was solved on a mesh. This approach enabled consistency with experimental results regarding changes in phase fractions.

Recently, the work by Chandrappa & Bernacki (2023) introduced a novel finite element level-set framework. The focus was on the simulation of diffusive phase transformations, in particular the austenite to ferrite transformation in polycrystalline materials. A key innovation was the use of a diffuse interface approach within the level-set method (Fig. 13). This allowed the avoidance of the need for explicit treatment of jump conditions at phase boundaries during solute diffusion.

The approach provided a unified and efficient modeling of solute partitioning and interface migration. The framework also included the possibility of simulating concurrent phenomena, such as grain growth and recrystallisation. In an article by Chandrappa & Bernacki (2024), the model was significantly extended to deal with ternary and more complex alloy systems. The authors included solute drag effects and introduced more advanced nucleation models. They also improved the numerical treatment of boundary conditions. In particular, they addressed the conservation of both diffusive and advective solute fluxes. The updated model was tested in large-scale simulations of microstructure evolution, and these improvements confirmed the potential of the level-set method.

Another recent work (Pohjonen, 2023) presents a hybrid computational approach that links the level-set concept with phase-field-like diffuse interfaces, illustrating how the strengths of different methods can be combined. The author modeled the transformations from austenite to ferrite (and also from austenite to bainite) during cooling. This approach treated the interface as a "diffuse field" but derived an advection equation for interface movement. In particular, it was shown that the formulation was reduced to the classical level-set equation in the limit of a narrow interface thickness. By incorporating transformation strains and carbon partitioning effects, this approach can naturally account for the invariant-plane strain shape change of bainite, as well as the volume change of ferrite.

The main limitation of this model is the selection of appropriate parameter values. While the author of this paper focused on showing how the presented model works, the selected parameters have no relation to the experimental data.

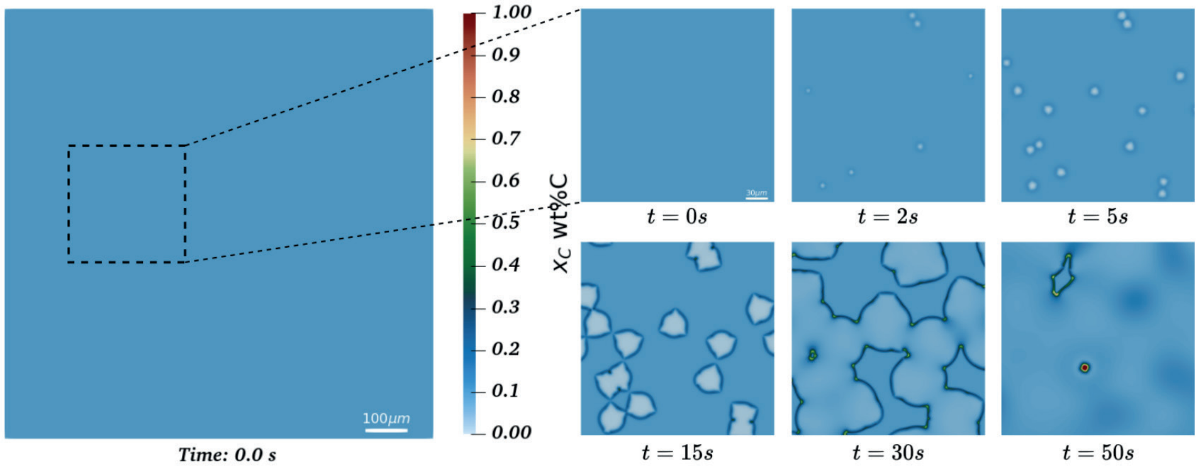

Fig. 13. Carbon diffusion in a two-phase system using the novel LS method (Chandrappa, 2024)

3.3. Monte Carlo models of austenite-to-ferrite Phase Transformations

Only a few research groups have modeled the diffusional austenite-ferrite transformation using Monte Carlo methods. Tong and co-workers (Tong et al., 2002, 2004a, 2004b, 2005) conducted extensive simulations for Fe-C and Fe-C-Mn steels. These 2D simulations successfully reproduced both the microstructure of nucleating ferrite and kinetic dependencies. Initially, Tong et al. (2002) introduced a two-dimensional Monte Carlo simulation utilizing a Landau–Ginzburg free-energy model, focusing primarily on the free-energy minimization and carbon diffusion within the austenite-ferrite system. This initial approach effectively predicted equilibrium volume fractions of phases and was experimentally validated. Subsequently, Tong et al. (2004a) introduced a mesoscale simulation employing a Q-state Potts model, incorporating continuous cooling conditions and a random-jump-based carbon diffusion model independent of numerical diffusion equations. This paper provided a detailed examination of interfacial energies and simulated the formation of polygonal ferrite grains and pearlite structures under varying cooling rates. Another work (Tong et al., 2004b) further expanded the model by modeling deformation-induced ferrite transformation (DIFT), incorporating deformation energy, dislocation densities, and recrystallization effects. This work uniquely examined oscillations in the volume fraction of ferrite, highlighting the effects of strain and strain rate, as well as the phenomenon of reverse transformation. Finally, Tong et al. (2005) refined the Q-state Potts model approach to investigate the transformation under non-equilibrium interface conditions, applying a mixed diffusion/interface-controlled mechanism. This model uniquely considered carbon diffusion within ferrite and analyzed the impact of carbon concentration and annealing temperature, employing a simplified constant-value interface energy model. Thus, each successive paper introduced new physical phenomena and refined modeling techniques, progressively enhancing the realism and complexity of simulations.

These 2D simulations on a hexagonal lattice successfully reproduced both the microstructure of precipitating ferrite and kinetic dependencies. It is worth noting that cementite was not explicitly modeled in these studies, meaning its inclusion would require expanding the number of phases and incorporating separate plates for cementite.

In subsequent years, hybrid approaches were employed, combining the Monte Carlo method with other discrete techniques. Xiao et al. (2006) developed a coupled mesoscale simulation that integrated the Crystal Plasticity Finite Element Method (CPFEM) with a Q-state Potts Monte Carlo method. This approach enabled a detailed study of the influence of plastic deformation of austenite on the subsequent ferrite formation. By incorporating stored deformation energy and crystallographic orientation data from CPFEM as initial conditions for the Monte Carlo simulation, this work revealed that plastic deformation accelerates transformation kinetics and increases the equilibrium ferrite fraction. The study emphasized that deformation-induced defects significantly enhance ferrite nucleation sites and examined the interplay between deformation and long-range carbon diffusion as well as short-range iron diffusion across the interface. In the same year, Bos et al. (2006) introduced a novel multi-lattice kinetic Monte Carlo (kMC) simulation specifically targeting the massive transformation from fcc (γ-austenite) to bcc (α-ferrite) iron. This method uniquely accounted for variable, individual atomic jump activation energies based on local atomic environments, as opposed to using constant energy barriers. This allowed detailed insight into the energetics of atomic jumps at the interphase boundary. The study concluded that transformation kinetics were governed by sequences of energetically unfavorable jumps of atom groups, forming intermediate states at the phase boundary.

Building upon these methodologies, Li et al. (2007) applied both deterministic cellular automata and probabilistic Potts Monte Carlo models to analyze ferrite grain growth modes in detail. Their simulations showed that the ferrite grain growth behavior is influenced by both "hard impingement," related to grain boundary interactions, and "soft impingement" resulting from overlapping carbon diffusion fields. This work identified multiple grain growth behaviours, including parabolic growth, delayed growth, and even temporary or permanent shrinkage of ferrite grains, phenomena that were partly confirmed by synchrotron X-ray experiments.

Later studies by Biglari & Mittemeijer (2013, 2014) further advanced understanding of the transformation under mechanical loading conditions using multi-lattice kinetic Monte Carlo simulations. Their research provided insights into how external uniaxial, planar, and hydrostatic stresses influence the massive transformation kinetics. It was found that the presence of stress significantly affects interface mobility, primarily by modifying local atomic arrangements required to unblock lattice sites for transformation. Specifically, compressive stresses accelerated the transformation, while tensile stresses slowed it down. Their work also highlighted the importance of vacancy concentrations at the interface. They demonstrated that local clusters of relaxed atoms surrounding vacancies strongly influence transformation kinetics and interfacial mobility under stress.

For MC modeling of austenite-ferrite transformations, the method has not been developed recently. However, currently, the method has found application especially in the direction of microstructure modeling under thermal loading, e.g. 3D printing, welding with different materials (Zhang Z. et al., 2022).

3.4. Cellular Automaton models of austenite-to-ferrite Phase Transformations

One of the first works in this area (Jacot & Rappaz, 1997) focused on the development of a 2D grain growth model for predicting microstructural evolution during continuous cooling. The authors presented a general two-phase approach that predicted diffusive phase transformations from ferrite to γ austenite, incorporating a hexagonal grid to solve the diffusion equation using the FDM approach. Special interface elements were introduced to account for boundary conditions at the moving interface between the two phases, such as equilibrium phase diagrams and solute flux balance. Each CA cell in this grid could represent a grain, and its carbon concentration and was updated at each time step based on the solution of the diffusion equation. When the phase fraction fell below zero, the CA cell was considered to be fully transformed. Kumar et al. (1998) developed a similar model to study the nucleation and growth of ferrite using a 2D square cell-based CA space. The model assumed that nucleation sites were distributed along the grain boundaries, each with an associated undercooling range. These sites became active at specific undercoolings, initiating nucleation without incubation time. The distribution of these sites followed a Gaussian function with three parameters determined by fitting to experimental data. Once activated, nuclei grew into austenite through diffusion-controlled growth. Then, Varma et al. (2001) proposed a modified model that successfully predicted ferrite grain size and volume fractions across different cooling rates. It incorporated the growth of pearlite and extended nucleation with time and temperature dependence. This model resulted in notable agreement between simulated and experimental results for 0.28% and 0.38% carbon steels. Furthermore, Zhang L. et al. (2003) developed a model based on the article by Jacot & Rappaz (1997) utilizing nucleation probability calculation. In this approach, nucleation occurred when undercooling happened, and the nucleation probability for each cell at the grain boundary was calculated using the nucleus density function. The solution incorporated the cooling rate and calculation of nucleation rate, which was based on physical parameters and differences in Gibbs energies. Finally, due to the limitations of the model, there was no possibility to quantitatively predict the ferrite grain growth kinetics (Lan Y. J. et al., 2004a, 2004b). The CA model presented by Kundu et al. (2004) incorporated nucleation and diffusion processes, with the FDM applied to solve the second Fick's law within the CA cells. They assumed 1D diffusion along the grain boundary and 2D diffusion within the grains. The nucleation model was based on calculating a number of new nuclei from the Classical Nucleation Theory (CNT) approach and placing them randomly at the boundary region. The growth mechanism of ferrite grains utilized mass balance to obtain velocity, and it was used to calculate the fractions of ferrite in cells.

The first CA-based model that introduced the austenite to ferrite transformation under non-equilibrium interface conditions was developed by Lan Y. J. et al. (2004a, 2004b). The authors included interface mobility in the form of a thermally activated function as a part of grain velocity calculations. The model used a driving force derived from the chemical potentials of specific elements at the interface. This work has been later extended to include deformed C-Mn steel during continuous cooling (Lan Y. J. et al., 2005a). The driving force was represented by a sum of chemical and stored deformation energies. The calculation of stored energy was primarily based on dislocation density, which was assumed to be homogeneous throughout the entire CA space for simplification purposes. In another work (Lan Y. J. et al., 2005b), the authors coupled this model with the crystal plasticity finite element model (CPFEM) to provide heterogeneously distributed deformation energy. Because ferrite nuclei emerge not only along austenite grain boundaries but also within austenite grain interiors where the stored deformation energy is high, the authors modified the nucleation model to incorporate this behavior.

Then, Bos et al. (2010) introduced a complex CA model to simulate the continuous annealing stage of ternary DP steels in a three-dimensional (3D) space. The approach consisted of a number of simplified submodels, including recrystallization, ferrite-austenite, and pearlite-austenite transformations upon heating, as well as austenite-ferrite transformation upon cooling. Each of them, despite the simplifications, did provide qualitatively accurate results. The extended version of this model was presented in the work by Mecozzi et al. (2011). Unlike the previous model, this one considered site-saturated nucleation during the austenite-ferrite transformation stage and incorporated the chemical concentration of substitution elements into the driving force calculation. Svyetlichnyy & Mikhalyov (2014) introduced a Frontal Cellular Automata (FCA) framework adapted to phase transformations in 3D space with a focus on nucleation to reduce the computational time. Contrary to the classical CA approach, in the FCA, the transfer of data between the CA cell its neighbouring cells is reversed. This approach reduced computational complexity but incorporated changes only at the front of the moving phase boundary. This model also considered only the transformation of austenite to ferrite and pearlite with low cooling rates, where grain growth is controlled by diffusion. Another interesting model is presented by Zheng et al. (2012). The authors of this work aimed to predict the behavior of austenite-to-ferrite and reverse transformations during cooling and deformation processes using the CA approach in 2D space. The research revealed that the transformation from retained austenite to ferrite and the reverse can occur simultaneously within the same material under specific conditions. Work presented in the work by Opara & Kuziak (2020) was designed to cover the decomposition of austenite into ferrite, bainite and martensite during continuous cooling. The authors have used a well-known and proven method of CA + FDM, and they successfully simulated these transformations for CP steel in 2D space. The simulations were performed using different cooling rates, from which it can be seen that the kinetic results deviate for particular rates. Nevertheless, these works show the potential of combining these methods.

Recently, various approaches have been increasingly used as a complement to CA-based models. One such interesting work is the article by Łach & Svyetlichnyy (2020), which is a combination of the FCA technique and the Lattice Boltzmann Method (LBM). The LBM is used to simulate carbon diffusion and heat flow. The authors have proved that the model works for 1D space for the austenite-to-ferrite transformation. In further work (Łach & Svyetlichnyy, 2023), the 3D heat flow model is developed using LBM and combined with the FCA method, where the grain growth process is controlled by temperature and the enthalpy of transformation. Sun et al. (2023) showed a different approach to simulate austenite-to-ferrite transformation, that is, a combination of CA with Bayesian Optimisation (BO), where the BO part is responsible for the automatic adjustment of the model parameters to the experimental data. This model is able to perform a simulation in isothermal conditions for 2D space with different initial carbon concentrations.

In the simulation of phase transformations, the CA method is an attractive choice for several reasons. The CA allows for effective modeling of large systems and is naturally suited to parallel computing, which facilitates simulations of large samples or long cooling times. Unlike the PF approach, which requires very large computational resources due to the need to use a fine mesh and solve costly differential equations. On the other hand, MC does not have a natural time scale and generates a high level of computational noise, making it more difficult to accurately reproduce real kinetic processes. CA, thanks to its neighborhood-based evolution rules, better reflects phase transformations and the dynamics of nucleation and growth. This method is also characterized by flexibility and expandability because it is based on simple rules which allow for the easy introduction of various physical mechanisms. Conversely, the LS and PF methods are more challenging to implement for multiphase or multigrain systems.

Therefore, this work focuses on the CA method, making use of its strengths and minimizing its weaknesses by incorporating it within a flexible architecture, which, together with the developed transition rules, allows for the simulation of complex phenomena at the phase boundaries.

4. Developed cellular automata model for γ → α transformation

As already mentioned, in this work, the CA method was selected as the main method to simulate the diffusive transformation from austenite to ferrite under continuous cooling conditions. Taking advantage of the fact that this method uses a regular, discrete space in the form of a grid, the finite difference method was also introduced. FDM is used to calculate changes in carbon concentration in the austenite region caused by diffusion over time. The entire coupled CA-FDM model was built using a modular structure, where each module represents a separate phenomenon: Nucleation, Diffusion, Grain growth, and Redistribution. During the simulation, global steps are performed with a certain time step. In each of these steps, every module is considered in turn and carries out its own iterations using a time step equal to or smaller than the global time step, as seen in Figure 14. The CA space is assumed to be 2D and composed of regularly distributed square CA cells. Each CA cell has a physical size, a state, and stores additional information such as element concentration and ferrite fraction. Available CA cell states are defined as follows: austenite (γ) and ferrite (α) and austenite/ferrite (α/γ), which marks a CA cell located at the phase boundary region (Fig. 15).

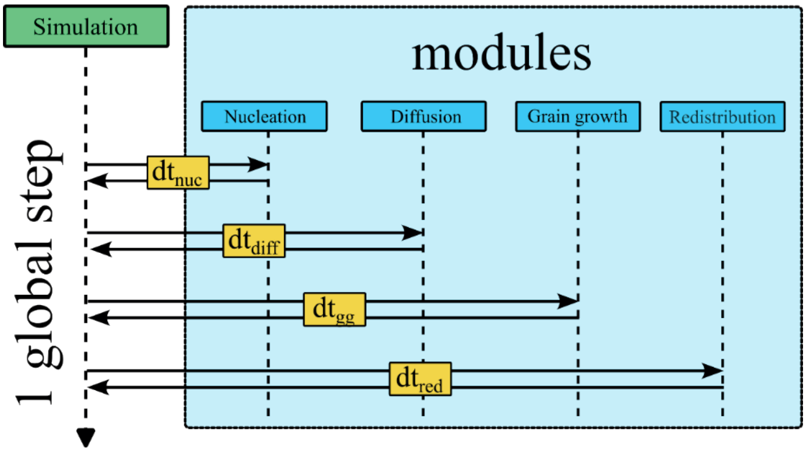

Fig. 14. Diagram of the developed modular CA-FDM model

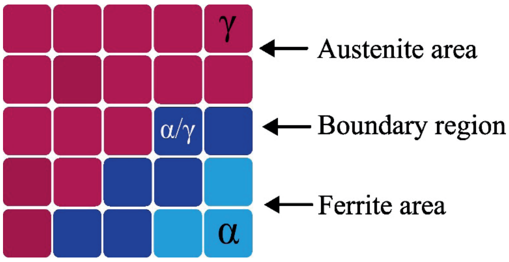

Fig. 15. Conceptual representation of the CA cells' states

The first module, Nucleation, is responsible for placing nuclei in the CA space. During the simulation, the probability p of nucleation (Eq. (1)) is calculated for each austenite cell. This probability depends on the value of undercooling, the local position (inside the grain, at the grain boundary, or at triple junctions), the ratio of the current austenite volume fraction to the initial state, and a Gaussian function. The shape and range of this function are fitted based on experimental results. For each investigated material, these model parameters must be identified:

$$p = \frac{a_1\, c\, dt \left(\frac{B_{curr}}{B_{init}}\right)^3 l}{1 + \exp\left(\frac{A_{e3} - T - a_2}{a_3}\right)} \tag{1}$$

where: c – cooling rate [K/s]; dt – time step [s]; T – current temperature [K]; A_{e3} – temperature at A_{e3} line in phase diagram; B_{curr} – current number of austenite cells; B_{init} – initial number of austenite cells; l – local position factor; a_1, a_2, a_3 – Gaussian function shape parameters.

The second module, Diffusion, is implemented to solve Fick's second law. The finite difference method, with a central scheme in space and a forward scheme in time (Eq. (2)) is used in this case. It is assumed that carbon diffusion mainly takes place in the austenite region, while it is neglected in the ferrite region. At the interface between phases, a von Neumann boundary condition is applied. The diffusion coefficient depends on temperature and activation energy. The module's time step is adjusted to meet the stability condition (Eq. (3)):

$$u_{i,j}^{t+1} = u_{i,j}^{t} + \frac{Ddt}{L_{ca}^2}\left(u_{i+1,j}^{t} + u_{i-1,j}^{t} + u_{i,j+1}^{t} + u_{i,j-1}^{t} - 4u_{i,j}^{t}\right) \tag{2}$$

$$dt \le \frac{L_{ca}^2}{4D} \tag{3}$$

$$D = D_o exp\left(-\frac{Q}{RT}\right) \tag{4}$$

where: u – element concentration [%]; t – step of simulation; D_o – diffusion coefficient [m^2/s]; Q – activation energy [J/mol]; L_{ca} – cells physical size [m]; R – gas constant [J/K·mol].

During the grain growth stage, the increments of ferrite inside boundary cells are calculated across the whole automaton space (Eq. (5)). These increments are then summed up in the neighboring austenite cells. The increases depend on the velocity of the phase boundary, which varies according to the local carbon concentration. This velocity comes from multiplying the boundary's mobility by the chemical driving force. The chemical driving force depends on how far the system is from equilibrium. At the same time, transition rules are used to simulate the movement of the boundary and, thus, the growth of ferrite grains (Eq. (6)):

$$df_\alpha = \frac{v}{L_{ca}}dt = \frac{MF}{L_{ca}}dt = \frac{M_0 D_0 \exp\left(-\frac{Q}{RT}\right) x\left(u_{eq}^{c}(T) - u^{c}\right)}{L_{ca}}dt \tag{5}$$

$$s_{i,j}^{t+1}=\begin{cases}Austenite/ferrite \leftrightarrow s_{i,j}^{t}=Austenite \wedge f_{\alpha_{i,j}} \geq 1\\ Austenite/ferrite \leftrightarrow s_{i,j}^{t}=Austenite \wedge s_{l,k}^{t}=Ferrite\\ Ferrite \leftrightarrow s_{i,j}^{t}=Austenite/ferrite \wedge s_{l,k}^{t} \neq Austenite\\ s_{i,j}^{t} \leftrightarrow otherwise\end{cases} \tag{6}$$

where: v – grain boundary velocity [m/s]; M – boundary mobility [m^{2}s/kg]; M_0 – mobility coefficient [m^{2}s/kg]; F – chemical driving force [J^3/m]; x – model coefficient [J^3/m]; u^c_{eq} – equilibrium carbon concentration [%]; u^c – carbon concentration of a cell [%]; i, j – investigated CA cell location; k, l – neighbors location of the investigated CA cell.

Redistribution related to carbon is a complementary module to the previous one. It is assumed that the boundary between ferrite and austenite is dimensionless. When a boundary cell evolves to ferrite, the surplus carbon remains in place. However, in reality, this carbon moves across the boundary into the austenite, and the developed redistribution module simulates that process. It calculates the carbon flux (Eq. (7)) from ferrite cells with surplus carbon into neighboring boundary cells. Then, based on this flux, the carbon is transferred until the ferrite cell reaches its equilibrium concentration:

$$J=\frac{v}{V}\left(u_{\alpha}^{c}-u_{\alpha eq}^{c}\right) \tag{7}$$

where: V – cell's volume; u^c_α – carbon concentration at ferrite cell; $u^c_{\alpha eq}$ – carbon equilibrium concentration in ferrite.

Test simulations were carried out to verify the functionality of the presented model. For this purpose, a 2D cellular automaton with a size of 300 × 300 CA cells was created, where the side length of a single cell is 1 μm. The initial temperature was set to 1103 K, and the initial carbon concentration in the austenite cells was 0.16%. The exemplary results presented in Figures 16–18 correspond to a cooling rate of 1 K/s.

Figure 16 represents the distribution of carbon in the simulated CA space. The resulting ferrite grains transport excess carbon across the phase boundary toward the austenite region. This carbon is partially carried over by a diffusion mechanism toward the center of the austenite grains, into areas with lower concentrations. Between the resulting grains (Fig. 17) at the end of the simulation, clusters of carbon with high concentration, close to the equilibrium value, were formed. These are the areas where future transformations (pearlitic and bainitic) will take place. The distribution of the nuclei presented in Figure 18 ensures the correctness of nucleation. Moreover, the introduced sub-models, grain growth and distribution, are capable of simulating the kinetics of ferrite grain growth, as shown in the same figure. The curve of ferrite fraction represents three stages of ferrite transformation:

1. initial nucleation and slow grain growth;
2. transformation start (approx. 5%) and dynamic growth of grains with diffusion of elements;
3. end of transformation (approx. 80%), where the microstructure has stabilized

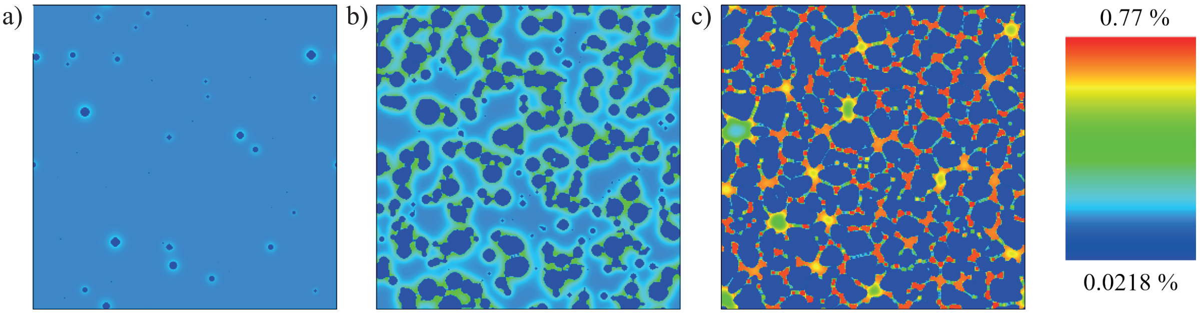

Fig. 16. Carbon concentration maps from the initial (a), middle (b), and final (c) stage of the austenite to ferrite transformation simulation

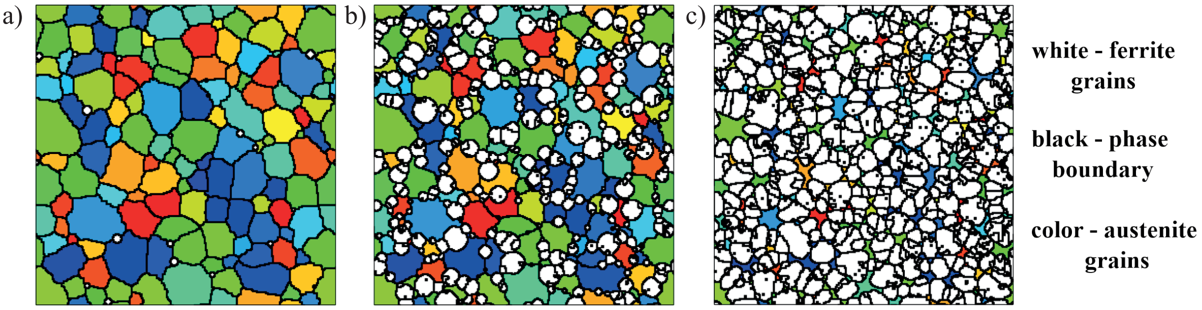

Fig. 17. Microstructure from the initial (a), middle (b), and final (c) stage of the austenite to ferrite transformation simulation

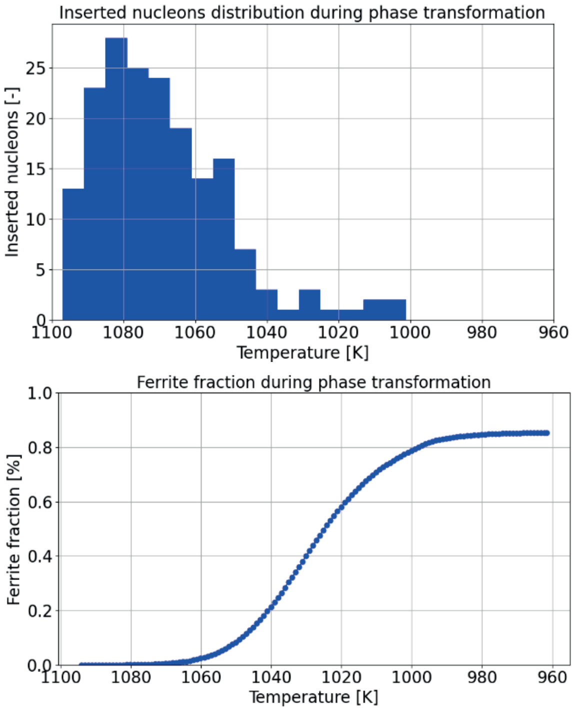

Fig. 18. The distribution of nuclei and evolution of ferrite fraction during the austenite to ferrite transformation

Additionally, Table 2 summarizes the individual results for the simulation and the results obtained from the experiment to confirm the model's validity.

Table 2. Summary of quantitative results for simulation and experiment for 1 K/s cooling rate

Source	Ferrite fraction [%]	Average ferrite grain diameter [μm]
Experiment	84.25	19.03
Simulation	85.38	18.70

As presented, the model is able to successfully simulate the austenite-ferrite transformation under continuous cooling. The applied CA method gives correct results, especially when the introduced modifications solved the main problems of this approach. However, it should be noted that this model has certain limitations. The driving force during transformation is calculated from the difference in carbon concentration, without considering other elements. Not considering substitution elements may cause the results for higher cooling rates, where bainitic and pearlitic transformations begin, to deviate significantly from the actual values. This is because at higher rates, interface-controlled transformation mode dominates, and substitution elements have a significant influence in this mode. Due to this factor, the presented model is capable of performing reliable simulations for rates lower than 10 K/s. These issues will be addressed during the further development stages of the model.

Conclusions

In recent years, significant progress has been made in modeling the phase transformation from austenite to ferrite in steels. Modern computational techniques, such as PF, LS, CA, or MC models, have enabled the detailed reproduction of microstructural evolution on a large scale, capturing phenomena like diffusion, nucleation, and particular transformation control modes.

A promising direction identified in the study is the development of hybrid methods combining the strengths of the aforementioned approaches. Such hybrid models, exemplified by the Cellular Automata-Finite Difference method used for γ → α transformations under continuous cooling, integrate discrete simulation with diffusion modeling. This approach demonstrates improved accuracy and computational efficiency, enhancing practical applicability.

Moreover, the study emphasizes the need for continuous improvement in computational efficiency, particularly addressing issues such as grid anisotropy in CA methods, the time dependence in MC simulations, and the high computational cost of PF methods, to expand their practical usability in more complex systems.

Acknowledgements

The work was undertaken within the framework of fundamental statutory research financed by the Ministry of Science and Higher Education, Grant No. 16.16.110.663. We would like to thank everyone who is involved in supporting the open access initiatives.

References

Barbe, F., & Quey, R. (2011). A numerical modelling of 3D polycrystal-to-polycrystal diffusive phase transformations involving crystal plasticity. *International Journal of Plasticity*, *27*(6), 823–840. https://doi.org/10.1016/j.ijplas.2010.09.008

Bengochea, R., López, B., Gutierrez, I. (1998). Microstructural evolution during the austenite-to-ferrite transformation from deformed austenite. *Metallurgical and Materials Transactions A*, *29*(2), 417–426. https://doi.org/10.1007/s11661-998-0122-1

Bernacki, M. (2024a). Kinetic equations and level-set approach for simulating solid-state microstructure evolutions at the mesoscopic scale: State of the art, limitations, and prospects. *Progress in Materials Science*, *142*, 101224. https://doi.org/10.1016/j.pmatsci.2023.101224

Bernacki, M. (2024b). Level-set method for the modeling of microstructure evolution. In M. Bernacki, S. Forest (Coordinators), *Digital Materials: Continuum Numerical Methods at the Mesoscopic Scale* (pp. 203–260). Wiley. https://doi.org/10.1002/9781394332489.ch6

Bhadeshia, H. K. D. H. (2010). Phase transformations contributing to the properties of modern steels. *Bulletin of the Polish Academy of Sciences: Technical Sciences*, *58*(2), 255–265. https://doi.org/10.2478/v10175-010-0024-4

Bhadeshia, H. K. D. H. (2021). *Theory of Transformations in Steels*. CRC Press.

Biglari, M., & Mittemeijer, E. J. (2013). Simulation of the massive austenite–ferrite transformation under uniaxial loading. *Computational Materials Science*, *77*, 214–223. https://doi.org/10.1016/j.commatsci.2013.04.041

Biglari, M., & Mittemeijer, E. J. (2014). Mobility of the austenite–ferrite interface under various states of loading. *Philosophical Magazine*, *94*(8), 801–813. https://doi.org/10.1080/14786435.2013.868941

Bos, C., Sommer, F., & Mittemeijer, E. J. (2006). Multi-lattice kinetic Monte Carlo simulation of interphase kinetics for an iron fcc to bcc transformation. *Modelling and Simulation in Materials Science and Engineering*, *14*(2), 273–282. https://doi.org/10.1088/0965-0393/14/2/010

Bos, C., Mecozzi, M. G., & Sietsma, J. (2010). A microstructure model for recrystallisation and phase transformation during the dual-phase steel annealing cycle. *Computational Materials Science*, *48*(3), 692–699. https://doi.org/10.1016/j.commatsci.2010.03.010

Bzowski, K., Rauch, Ł., Pietrzyk, M., Kwiecień, M., & Muszka, K. (2021). Numerical modeling of phase transformations in dual-phase steels using level set and SSRVE approaches. *Materials*, *14*(18), 5363. https://doi.org/10.3390/ma14185363

Cha, P.-R., Kim, J.-Y., Kim, W.-T., & Kim, S. G. (2010). Phase field study on the austenite/ferrite transition in low carbon steel. *Materials and Manufacturing Processes*, *25*(1–3), 106–110. https://doi.org/10.1080/10426910903153166

Chafia, Z., Yvonnet, J., Bleyer, J., Vincent, S., & El Ouafa, S. (2024). Massively parallel phase field fracture simulations on supercomputers: Towards multi-billion degree-of-freedom computations. *Advanced Modeling and Simulation in Engineering Sciences*, *11*(1), 25. https://doi.org/10.1186/s40323-024-00280-4

Chandrappa, N. (2024). *A Global Level-Set Based Full-Field Numerical Framework to Simulate Diffusive Solid-State Phase Transformation in Polycrystalline Metallic Materials* [PhD thesis, Université Paris Sciences et Lettres]. ParisTech. https://pastel.hal.science/tel-04702550

Chandrappa, N., & Bernacki, M. (2023). A level-set formulation to simulate diffusive solid/solid phase transformation in polycrystalline metallic materials – Application to austenite decomposition in steels. *Computational Materials Science*, *216*, 111840. https://doi.org/10.1016/j.commatsci.2022.111840

Chandrappa, N., & Bernacki, M. (2024). High-fidelity level-set modeling of diffusive solid-state phase transformations for polycrystalline materials. *Computational Materials Science*, *243*, 113142. https://doi.org/10.1016/j.commatsci.2024.113142

Cheloee Darabi, A., Rastgordani, S., Khoshbin, M., Guski, V., & Schmauder, S. (2023). Hybrid data-driven deep learning framework for material mechanical properties prediction with the focus on dual-phase steel microstructures. *Materials*, *16*(1), 447. https://doi.org/10.3390/ma16010447

Chen, H., & Zwaag, S., van der (2014). A general mixed-mode model for the austenite-to-ferrite transformation kinetics in Fe–C–M alloys. *Acta Materialia*, *72*, 1–12. https://doi.org/10.1016/j.actamat.2014.03.034

Chen, H., Liu, Y., Yan, Z., Li, Y., & Zhang, L. (2010). Consideration of the growth mode in isochronal austenite-ferrite transformation of ultra-low-carbon Fe–C alloy. *Applied Physics A*, *98*(1), 211–217. https://doi.org/10.1007/s00339-009-5375-z

Chen, L.-Q. (2002). Phase-Field Models for Microstructure Evolution. *Annual Review of Materials Research*, *32*(1), 113–140. https://doi.org/10.1146/annurev.matsci.32.112001.132041

Chen, L.-Q., & Zhao, Y. (2022). From classical thermodynamics to phase-field method. *Progress in Materials Science*, *124*, 100868. https://doi.org/10.1016/j.pmatsci.2021.100868

Deffrennes, G., Terayama, K., Abe, T., Ogamino, E., & Tamura, R. (2023). A framework to predict binary liquidus by combining machine learning and CALPHAD assessments. *Materials & Design*, *232*, 112111. https://doi.org/10.1016/j.matdes.2023.112111

Enomoto, M., Kamiya, M., & Nagai, T. (1996). Computer simulation of two-dimensional grain growth with anisotropic grain boundary energy and mobility by vertex model. *Materials Science Forum*, *204–206*, 71–82. https://doi.org/10.4028/www.scientific.net/MSF.204-206.71

Ervik, Å., Lervåg, K. Y., & Munkejord, S. T. (2014). A robust method for calculating interface curvature and normal vectors using an extracted local level set. *Journal of Computational Physics*, *257*(A), 259–277. https://doi.org/10.1016/j.jcp.2013.09.053

Fuchizaki K., & Kawasaki K. (1995). Time evolution of three-dimensional cellular systems: Computer modeling based on vertex-type models. *Physica A: Statistical Mechanics and Its Applications*, *221*(1–3), 202–215. https://doi.org/10.1016/0378-4371(95)00224-U

Furuhara, T., Kikumoto, K., Saito, H., Sekine, T., Ogawa, T., Morito, S., & Maki, T. (2008). Phase transformation from fine-grained austenite. *ISIJ International*, *48*(8), 1038–1045. https://doi.org/10.2355/isijinternational.48.1038

Gamsjäger, E., Militzer, M., Fazeli, F., Svoboda, J., & Fischer, F. D. (2006). Interface mobility in case of the austenite-to-ferrite phase transformation. *Computational Materials Science*, *37*(1–2), 94–100. https://doi.org/10.1016/j.commatsci.2005.12.011

Gaude-Fugarolas, D., & Bhadeshia, H. K. D. H. (2003). A model for austenitisation of hypoeutectoid steels. *Journal of Materials Science*, *38*(6), 1195–1201. https://doi.org/10.1023/A:1022805719924

Gawąd, J., Paszyński, M., Matuszyk, P., & Madej, L. (2008). Cellular automata coupled with HP-adaptive Finite Element Method applied to simulation of austenite-ferrite phase transformation with a moving interface. In M. Pietrzyk et al. (Eds.), *Metal Forming 2008. Proceedings of the 12th International Conference on Metal Forming, Akademia Górniczo-Hutnicza, Kraków, Poland* (vol. 2, pp. 579–586). Verlag Stahleisen.

Ghosh, S., Newman, C. K., & Francois, M. M. (2022). Tusas: A fully implicit parallel approach for coupled phase-field equations. *Journal of Computational Physics*, *448*, 110734. https://doi.org/10.1016/j.jcp.2021.110734

Ghumman, U. F., Fang, L., Wagner, G. J., & Chen, W. (2023). Calibration of Cellular Automaton Model for Microstructure Prediction in Additive Manufacturing Using Dissimilarity Score. *Journal of Manufacturing Science and Engineering*, *145*(6), 061002. https://doi.org/10.1115/1.4056690

Gomez, H., Bures, M., & Moure, A. (2019). A review on computational modelling of phase-transition problems. *Philosophical Transactions of the Royal Society A: Mathematical, Physical and Engineering Sciences*, *377*(2143), 20180203. https://doi.org/10.1098/rsta.2018.0203

Gouné, M., Danoix, F., Ågren, J., Bréchet, Y., Hutchinson, C. R., Militzer, M., Purdy, G., Zwaag, S., van der, & Zurob, H. (2015). Overview of the current issues in austenite to ferrite transformation and the role of migrating interfaces therein for low alloyed steels. *Materials Science and Engineering: R: Reports*, *92*, 1–38. https://doi.org/10.1016/j.mser.2015.03.001

Hackenberg, R. E. (2012). 1 – The historical development of phase transformations understanding in ferrous alloys. In E. Pereloma, D. V. Edmonds (Eds.), *Phase Transformations in Steels* (vol. 1: *Fundamentals and Diffusion-Controlled Transformations*, pp. 3–55). Woodhead Publishing. https://doi.org/10.1533/9780857096104.1.3

Hallberg, H. (2011). Approaches to modeling of recrystallization. *Metals*, *1*(1), 16–48. https://doi.org/10.3390/met1010016

Hallberg, H., Håkansson, P., & Ristinmaa, M. (2010). Thermo-mechanically coupled model of diffusionless phase transformation in austenitic steel. *International Journal of Solids and Structures*, *47*(11–12), 1580–1591. https://doi.org/10.1016/j.ijsolstr.2010.02.019

Hansen, P. B. (1993). Parallel cellular automata: A model program for computational science. *Concurrency: Practice and Experience*, *5*(5), 425–448. https://doi.org/10.1002/cpe.4330050504

Hillert, M. (1999). Solute drag, solute trapping and diffusional dissipation of Gibbs energy. *Acta Materialia*, *47*(18), 4481–4505. https://doi.org/10.1016/S1359-6454(99)00336-5

Hodgson, P. D., Beladi, H., & Kelly, G. L. (2005). The development of ultrafine grained steels through thermomechanical processing. *Canadian Metallurgical Quarterly*, *44*(2), 179–186. https://doi.org/10.1179/cmq.2005.44.2.179

Hu, Y., Wang, K., & Spatschek, R. (2024). A data-driven strategy for phase field nucleation modeling. *Npj Materials Degradation*, *8*(1), 109. https://doi.org/10.1038/s41529-024-00529-8

Huang, C.-J., Browne, D. J., & McFadden, S. (2006). A phase-field simulation of austenite to ferrite transformation kinetics in low carbon steels. *Acta Materialia*, *54*(1), 11–21. https://doi.org/10.1016/j.actamat.2005.08.033

Iwamoto, T., Cherkaoui, M., & Busso, E. P. (2008). A finite element-based level-set method of an interface motion driven by a diffusion field: Application to a phase transformation problem. *Computational Materials Science*, *44*(2), 792–801. https://doi.org/10.1016/j.commatsci.2008.05.030

Jacobsson, E., Hallberg, H., Hektor, J., Iyengar, S., & Ristinmaa, M. (2024). A level set approach to modelling diffusional phase transformations under finite strains with application to the formation of Cu 6 Sn 5. *Computational Materials Science*, *244*, 113284. https://doi.org/10.1016/j.commatsci.2024.113284

Jacot, A., & Rappaz, M. (1997). A two-dimensional diffusion model for the prediction of phase transformations: Application to austenitization and homogenization of hypoeutectoid Fe-C steels. *Acta Materialia*, *45*(2), 575–585. https://doi.org/10.1016/S1359-6454(96)00199-1

Kawasaki, K., Nagai, T., & Nakashima, K. (1989). Vertex models for two-dimensional grain growth. *Philosophical Magazine B*, *60*(3), 399–421. https://doi.org/10.1080/13642818908205916

Khedkar, K., Mamaghani, A. C., Ghysels, P., Patankar, N. A., & Bhalla, A. P. S. (2025). Preventing mass loss in the standard level set method: New insights from variational analyses. *Journal of Computational Physics*, *520*, 113495. https://doi.org/10.1016/j.jcp.2024.113495

Kobayashi, R. (1993). Modeling and numerical simulations of dendritic crystal growth. *Physica D: Nonlinear Phenomena*, *63*(3–4), 410–423. https://doi.org/10.1016/0167-2789(93)90120-P

Krielaart, G. P., Sietsma, J., & Zwaag, S., van der (1997). Ferrite formation in Fe-C alloys during austenite decomposition under non-equilibrium interface conditions. *Materials Science and Engineering: A*, *237*(2), 216–223. https://doi.org/10.1016/S0921-5093(97)00365-1

Kumar, M., Sasikumar, R., & Kesavan Nair, P. (1998). Competition between nucleation and early growth of ferrite from austenite—Studies using cellular automaton simulations. *Acta Materialia*, *46*(17), 6291–6303. https://doi.org/10.1016/S1359-6454(98)00243-2

Kundu, S., Dutta, M., Ganguly, S., & Chandra, S. (2004). Prediction of phase transformation and microstructure in steel using cellular automaton technique. *Scripta Materialia*, *50*(6), 891–895. https://doi.org/10.1016/j.scriptamat.2003.12.007

Łach, Ł., & Svyetlichnyy, D. (2020). Development of hybrid model for modeling of diffusion phase transformation. *Engineering Computations*, *37*(8), 2761–2783. https://doi.org/10.1108/EC-02-2019-0059

Łach, Ł., & Svyetlichnyy, D. (2023). 3D model of heat flow during diffusional phase transformations. *Materials*, *16*(13), 4865. https://doi.org/10.3390/ma16134865

Lan, Y. J., Li, D. Z., Huang, C. J., & Li, Y. Y. (2004a). A cellular automaton model for austenite to ferrite transformation in carbon steel under non-equilibrium interface conditions. *Modelling and Simulation in Materials Science and Engineering*, *12*(4), 719–729. https://doi.org/10.1088/0965-0393/12/4/012

Lan, Y. J., Li, D. Z., & Li, Y. Y. (2004b). Modeling austenite–ferrite transformation in low carbon steel using the cellular automaton method. *Journal of Materials Research*, *19*(10), 2877–2886. https://doi.org/10.1557/JMR.2004.0397

Lan, Y. J., Li, D. Z., & Li, Y. Y. (2005a). Mesoscale simulation of ferrite transformation from deformed austenite during continuous cooling in a C–Mn steel using a cellular automaton method. *Computational Materials Science*, *32*(2), 147–155. https://doi.org/10.1016/j.commatsci.2004.07.005

Lan, Y. J., Xiao, N. M., Li, D. Z., & Li, Y. Y. (2005b). Mesoscale simulation of deformed austenite decomposition into ferrite by coupling a cellular automaton method with a crystal plasticity finite element model. *Acta Materialia*, *53*(4), 991–1003. https://doi.org/10.1016/j.actamat.2004.10.045

Lépinoux, J., Weygand, D., & Verdier, M. (2010). Modeling grain growth and related phenomena with vertex dynamics. *Comptes Rendus. Physique*, *11*(3–4), 265–273. https://doi.org/10.1016/j.crhy.2010.07.015

Lervåg, K. Y., & Ervik, Å. (2013). Curvature calculations for the level-set method. In A. Cangiani, R. L. Davidchack, E. Georgoulis, A. N. Gorban, J. Levesley, M. V. Tretyakov (Eds.), *Numerical Mathematics and Advanced Applications 2011: Proceedings of ENUMATH 2011, the 9th European Conference on Numerical Mathematics and Advanced Applications, Leicester, September 2011* (pp. 209–217). Springer Berlin, Heidelberg. https://doi.org/10.1007/978-3-642-33134-3_23

Leeuwen, Y., van, Sietsma, J., & Zwaag, S., van der (2003). The influence of carbon diffusion on the character of the γ–α phase transformation in steel. *ISIJ International*, *43*(5), 767–773.

Li, D. Z., Xiao, N. M., Lan, Y. J., Zheng, C. W., & Li, Y. Y. (2007). Growth modes of individual ferrite grains in the austenite to ferrite transformation of low carbon steels. *Acta Materialia*, *55*(18), 6234–6249. https://doi.org/10.1016/j.actamat.2007.07.041

Liang, C., Song, G., Wang, W., Sohn, I., & Zeng, J. (2024). In situ observation of the austenite to ferrite transformation in low-carbon steels from different initial phases at defined cooling rates. *Journal of Materials Research and Technology*, *28*, 2116–2126. https://doi.org/10.1016/j.jmrt.2023.12.157

Liang, X., Bos, C., Hermans, M., & Richardson, I. (2023). An Improved Cellular Automata Solidification Model Considering Kinetic Undercooling. *Metallurgical and Materials Transactions B*, *54*(3), 1088–1098. https://doi.org/10.1007/s11663-023-02742-3

Liu, C., Garner, A., Zhao, H., Prangnell, P. B., Gault, B., Raabe, D., & Shanthraj, P. (2021). CALPHAD-informed phase-field modeling of grain boundary microchemistry and precipitation in Al-Zn-Mg-Cu alloys. *Acta Materialia*, *214*, 116966. https://doi.org/10.1016/j.actamat.2021.116966

Liu, Y., Sommer, F., & Mittemeijer, E. (2006). The austenite–ferrite transformation of ultralow-carbon Fe–C alloy; transition from diffusion- to interface-controlled growth. *Acta Materialia*, *54*(12), 3383–3393. https://doi.org/10.1016/j.actamat.2006.03.029

Loginova, I., Odqvist, J., Amberg, G., & Ågren, J. (2003). The phase-field approach and solute drag modeling of the transition to massive γ → α transformation in binary Fe-C alloys. *Acta Materialia*, *51*(5), 1327–1339. https://doi.org/10.1016/S1359-6454(02)00527-X

Loginova, I., Ågren, J., & Amberg, G. (2004). On the formation of Widmanstätten ferrite in binary Fe–C – phase-field approach. *Acta Materialia*, *52*(13), 4055–4063. https://doi.org/10.1016/j.actamat.2004.05.033

Madej, L., Sitko, M., & Pietrzyk, M. (2016). Perceptive comparison of mean and full field dynamic recrystallization models. *Archives of Civil and Mechanical Engineering*, *16*(4), 569–589. https://doi.org/10.1016/j.acme.2016.03.010

Málek, M., Mičian, M., & Moravec, J. (2020). Determination of phase transformation temperatures by dilatometric test of S960MC steel. *Archives of Foundry Engineering*, *21*(2), 57–64. https://doi.org/10.24425/afe.2021.136098

Marek, M. (2013). Grid anisotropy reduction for simulation of growth processes with cellular automaton. *Physica D: Nonlinear Phenomena*, *253*, 73–84. https://doi.org/10.1016/j.physd.2013.03.005

Mason, J. K., Lind, J., Li, S. F., Reed, B. W., & Kumar, M. (2015). Kinetics and anisotropy of the Monte Carlo model of grain growth. *Acta Materialia*, *82*, 155–166. https://doi.org/10.1016/j.actamat.2014.08.063

Mamivand, M., Zaeem, M. A., El Kadiri, H., & Chen, L.-Q. (2013). Phase field modeling of the tetragonal-to-monoclinic phase transformation in zirconia. *Acta Materialia*, *61*(14), 5223–5235. https://doi.org/10.1016/j.actamat.2013.05.015

Mecozzi, M. G., Sietsma, J., & Zwaag, S., van der (2005). Phase field modelling of the interfacial condition at the moving interphase during the γ→α transformation in C–Mn steels. *Computational Materials Science*, *34*(3), 290–297. https://doi.org/10.1016/j.commatsci.2005.03.002

Mecozzi, M. G., Militzer, M., Sietsma, J., & Zwaag, S., van der (2008). The role of nucleation behavior in phase-field simulations of the austenite to ferrite transformation. *Metallurgical and Materials Transactions A*, *39*(6), 1237–1247. https://doi.org/10.1007/s11661-008-9517-2

Mecozzi, M. G., Bos, C., & Sietsma, J. (2011). 3D cellular automata modelling of solid–state transformations relevant in low–alloy steel production. *Solid State Phenomena*, *172–174*, 1140–1145. https://doi.org/10.4028/www.scientific.net/SSP.172-174.1140

Militzer, M., Mecozzi, M. G., Sietsma, J., & Zwaag, S., van der (2006). Three-dimensional phase field modelling of the austenite-to-ferrite transformation. *Acta Materialia*, *54*(15), 3961–3972. https://doi.org/10.1016/j.actamat.2006.04.029

Moelans, N., Blanpain, B., & Wollants, P. (2008). An introduction to phase-field modeling of microstructure evolution. *Calphad*, *32*(2), 268–294. https://doi.org/10.1016/j.calphad.2007.11.003

Mourad, H. M., & Garikipati, K. (2006). Advances in the numerical treatment of grain-boundary migration: Coupling with mass transport and mechanics. *Computer Methods in Applied Mechanics and Engineering*, *196*(1–3), 595–607. https://doi.org/10.1016/j.cma.2006.06.005

Murgas, B., Flipon, B., Bozzolo, N., & Bernacki, M. (2022). Level-set modeling of grain growth in 316L stainless steel under different assumptions regarding grain boundary properties. *Materials*, *15*(7), 2434. https://doi.org/10.3390/ma15072434

Mushongera, L. T., Kubendran Amos, P. G., Nestler, B., & Ankit, K. (2018). Phase-field simulations of pearlitic divergence in Fe-C-Mn steels. *Acta Materialia*, *150*, 78–87. https://doi.org/10.1016/j.actamat.2018.02.059

Mushongera, L. T., Kubendran Amos, P. G., Schoof, E., Kumar, P., & Nestler, B. (2020). The non-steady-state growth of divergent pearlite in Fe–C–Mn steels: A phase-field investigation. *Journal of Materials Science*, *55*(12), 5280–5295. https://doi.org/10.1007/s10853-019-04307-9

Ning, H., Qian, S., & Zhou, T. (2023). Applications of level set method in computational fluid dynamics: A review. *International Journal of Hydromechatronics*, *6*(1), 1. https://doi.org/10.1504/IJHM.2023.129126

Olshanskii, M., Reusken, A., & Schwering, P. (2024). *A narrow band finite element method for the level set equation* (no. arXiv: 2407.02950). arXiv. https://doi.org/10.48550/arXiv.2407.02950

Opara, J., & Kuziak, R. (2020). Study of phase transformations in complex phase steel using a mesoscale cellular automaton model Part I: Modeling Fundamentals. *Journal of Metallic Materials*, *72*(3), 17–31.

Osher, S., & Fedkiw, R. P. (2001). Level set methods: An overview and some recent results. *Journal of Computational Physics*, *169*(2), 463–502. https://doi.org/10.1006/jcph.2000.6636

Osher, S., & Sethian, J. A. (1988). Fronts propagating with curvature-dependent speed: Algorithms based on Hamilton-Jacobi formulations. *Journal of Computational Physics*, *79*(1), 12–49. https://doi.org/10.1016/0021-9991(88)90002-2

Osher, S., & Tsai, R. (2003). Level set methods and their applications in image science. *Communications in Mathematical Sciences*, *1*(4), 1–20. https://doi.org/10.4310/CMS.2003.v1.n4.a1

Pariser, G., Schaffnit, P., Steinbach, I., & Bleck, W. (2001). Simulation of the γ-α-transformation using the phase-field method. *Steel Research*, *72*(9), 354–360. https://doi.org/10.1002/srin.200100130

Pohjonen, A. (2023). Full field model describing phase front propagation, transformation strains, chemical partitioning, and diffusion in solid–solid phase transformations. *Advanced Theory and Simulations*, *6*(3), 2200771. https://doi.org/10.1002/adts.202200771

Preis, T., Virnau, P., Paul, W., & Schneider, J. J. (2009). GPU accelerated Monte Carlo simulation of the 2D and 3D Ising model. *Journal of Computational Physics*, *228*(12), 4468–4477. https://doi.org/10.1016/j.jcp.2009.03.018

Qin, R. S., & Bhadeshia, H. K. (2010). Phase field method. *Materials Science and Technology*, *26*(7), 803–811. https://doi.org/10.1179/174328409X453190

Raabe, D. (2000). Scaling Monte Carlo kinetics of the Potts model using rate theory. *Acta Materialia*, *48*(7), 1617–1628. https://doi.org/10.1016/S1359-6454(99)00451-6

Rozo Vasquez, J., Arian, B., Kersting, L., Homberg, W., Trächtler, A., & Walther, F. (2023). Detection of phase transformation during plastic deformation of metastable austenitic steel AISI 304L by means of X-ray diffraction pattern analysis. *Metals*, *13*(6), 1007. https://doi.org/10.3390/met13061007

Sarkar, P. (2000). A brief history of cellular automata. *ACM Computing Surveys*, *32*(1), 80–107. https://doi.org/10.1145/349194.349202

Scholtes, B., Ilin, D., Settefrati, A., Bozzolo, N., Agnoli, A., & Bernacki, M. (2016). Full field modeling of the Zener pinning phenomenon in a level set framework – discussion of classical limiting mean grain size equation. In M. Hardy, E. Huron, U. Glatzel, B. Griffin, B. Lewis, C. Rae, V. Seetharaman, S. Tin (Eds.), *Superalloys 2016. Proceedings of the 13th International Symposium on Superalloys* (pp. 497–503). Wiley. https://doi.org/10.1002/9781119075646.ch53

Schönfisch, B., & de Roos, A. (1999). Synchronous and asynchronous updating in cellular automata. *Biosystems*, *51*(3), 123–143. https://doi.org/10.1016/S0303-2647(99)00025-8

Schoof, E., Schneider, D., Streichhan, N., Mittnacht, T., Selzer, M., & Nestler, B. (2018). Multiphase-field modeling of martensitic phase transformation in a dual-phase microstructure. *International Journal of Solids and Structures*, *134*, 181–194. https://doi.org/10.1016/j.ijsolstr.2017.10.032

Shi, L., Xu, S., Lu, H., Chen, C., Shuai, S., Hu, T., Kao, A., Wang, J., & Ren, Z. (2022). A High-efficiency Virtual Submesh Cellular Automata Method for Solidification Simulation with Low Mesh Anisotropy. *ISIJ International*, *62*(8), 1674–1683. https://doi.org/10.2355/isijinternational.ISIJINT-2022-066

Shirzad, K., & Viney, C. (2023). A critical review on applications of the Avrami equation beyond materials science. *Journal of The Royal Society Interface*, *20*(203), 20230242. https://doi.org/10.1098/rsif.2023.0242

Sietsma, J. (2012). 14 – Nucleation and growth during the austenite-to-ferrite phase transformation in steels after plastic deformation. In E. Pereloma, D. V. Edmonds (Eds.), *Phase Transformations in Steels* (vol. 1: *Fundamentals and Diffusion-Controlled Transformations*, pp. 505–526). Woodhead Publishing. https://doi.org/10.1533/9780857096104.4.505

Sietsma, J., & Zwaag, S., van der (2004). A concise model for mixed-mode phase transformations in the solid state. *Acta Materialia*, *52*(14), 4143–4152. https://doi.org/10.1016/j.actamat.2004.05.027

Sitko, M., & Madej, Ł. (2016). Evaluation of efficient computational work division in parallel Monte Carlo grain growth algorithm. *Computer Methods in Materials Science*, *16*(3), 113–120. https://doi.org/10.7494/cmms.2016.3.0579

Sitko, M., & Madej, L. (2021). The role of the cellular automata cell size and time step length in the microstructure evolution model – The static recrystallization case study. *Journal of Computational Science*, *54*, 101437. https://doi.org/10.1016/j.jocs.2021.101437

Spencer, P. J. (2008). A brief history of CALPHAD. *Calphad*, *32*(1), 1–8. https://doi.org/10.1016/j.calphad.2007.10.001

Sun, F., Mino, Y., Ogawa, T., Chen, T.-T., Natsume, Y., & Adachi, Y. (2023). Evaluation of austenite–ferrite phase transformation in carbon steel using bayesian optimized cellular automaton simulation. *Materials*, *16*(21), 6922. https://doi.org/10.3390/ma16216922

Suwanpinij, P., Rudnizki, J., Prahl, U., & Bleck W. (2009). Investigation of the effect of deformation on γ-α phase transformation kinetics in hot-rolled dual phase steel by phase field approach. *Steel Research International*, *80*(9), 616–622. https://doi.org/10.2374/SRI09SP047

Svoboda, J., Fischer, F. D., Fratzl, P., Gamsjäger, E., & Simha, N. K. (2001). Kinetics of interfaces during diffusional transformations. *Acta Materialia*, *49*(7), 1249–1259. https://doi.org/10.1016/S1359-6454(01)00012-X

Svyetlichnyy, D. S., & Mikhalyov, A. I. (2014). Three-dimensional frontal cellular automata model of microstructure evolution – phase transformation module. *ISIJ International*, *54*(6), 1386–1395. https://doi.org/10.2355/isijinternational.54.1386

Syha, M., & Weygand, D. (2010). A generalized vertex dynamics model for grain growth in three dimensions. *Modelling and Simulation in Materials Science and Engineering*, *18*(1), 015010. https://doi.org/10.1088/0965-0393/18/1/015010

Szeliga, D., Bzowski, K., Rauch, Ł., Kuziak, R., & Pietrzyk, M. (2020). Mean field and full field modelling of microstructure evolution and phase transformations during hot forming and cooling of low carbon steels. *Computer Methods in Materials Science*, *20*(3). https://doi.org/10.7494/cmms.2020.3.0727

Thiessen, R. G., Sietsma, J., Palmer, T. A., Elmer, J. W., & Richardson, I. M. (2007). Phase-field modelling and synchrotron validation of phase transformations in martensitic dual-phase steel. *Acta Materialia*, *55*(2), 601–614. https://doi.org/10.1016/j.actamat.2006.08.053

Tong, M., Li, D., Li, Y., & Ni, J. (2002). Modeling the austenite-ferrite isothermal transformation in an Fe-C binary system and experimental verification. *Metallurgical and Materials Transactions A*, *33*(10), 3111–3115. https://doi.org/10.1007/s11661-002-0295-y

Tong, M., Li, D., & Li, Y. (2004a). Modeling the austenite–ferrite diffusive transformation during continuous cooling on a mesoscale using Monte Carlo method. *Acta Materialia*, *52*(5), 1155–1162. https://doi.org/10.1016/j.actamat.2003.11.006

Tong, M., Li, D., Li, Y., Ni, J., & Zhang, Y. (2004b). Monte Carlo-method simulation of the deformation-induced ferrite transformation in the Fe-C system. *Metallurgical and Materials Transactions A*, *35*(5), 1565–1577. https://doi.org/10.1007/s11661-004-0263-9

Tong, M., Li, D., & Li, Y. (2005). A q-state Potts model-based Monte Carlo method used to model the isothermal austenite-ferrite transformation under non-equilibrium interface condition. *Acta Materialia*, *53*(5), 1485–1497. https://doi.org/10.1016/j.actamat.2004.12.002

Torres, C., Emelianenko, M., Golovaty, D., Kinderlehrer, D., & Ta'asan, S. (2015). *Numerical analysis of the vertex models for simulating grain boundary networks* (no. arXiv:1410.5809). arXiv. https://doi.org/10.48550/arXiv.1410.5809

Tourret, D., Liu, H., & LLorca, J. (2022). Phase-field modeling of microstructure evolution: Recent applications, perspectives and challenges. *Progress in Materials Science*, *123*, 100810. https://doi.org/10.1016/j.pmatsci.2021.100810

Ubhi, H. S., Parsons, J., Othen, N., Campbell, S., Poole, R., & Gholinia, A. (2014). In-situ EBSD phase transformation and recrystallisation. *Journal of Physics: Conference Series*, *522*, 012011. https://doi.org/10.1088/1742-6596/522/1/012011

Van der Ven, A., & Delaey, L. (1996). Models for precipitate growth during the $\gamma \rightarrow \alpha + \gamma$ transformation in Fe–C and Fe–C–M alloys. *Progress in Materials Science*, *40*(3), 181–264. https://doi.org/10.1016/0079-6425(96)00002-3

Varma, M. R., Sasikumar, R., Pillai, S. G. K., & Nair, P. K. (2001). Cellular automaton simulation of microstructure evolution during austenite decomposition under continuous cooling conditions. *Bulletin of Materials Science*, *24*(3), 305–312. https://doi.org/10.1007/BF02704927

Wang, B. X., Liu, X. H., & Wang, G. D. (2009). Effect of deformation of austenite and cooling rates on transformation microstructures in a Mn–Cr gear steel. *Materials & Design*, *30*(6), 2198–2204. https://doi.org/10.1016/j.matdes.2008.08.021

Wang, K., Wu, H., Lv, S., Dong, L., Zhang, C., Wang, S., Wu, G., Gao, J., Zhu, J., & Mao, X. (2025). Multiphase field modeling of austenite to pearlite–ferrite transformation in hypoeutectoid steel. *International Journal of Minerals, Metallurgy and Materials*, *32*(6), 1427–1440. https://doi.org/10.1007/s12613-024-2993-6

Wei, L., Lin, X., Wang, M., & Huang, W. (2016). Low artificial anisotropy cellular automaton model and its applications to the cell-to-dendrite transition in directional solidification. *Materials Discovery*, *3*, 17–28. https://doi.org/10.1016/j.md.2016.06.001

Weigel, M. (2017). *Monte Carlo methods for massively parallel computers* (no. arXiv:1709.04394). arXiv. https://doi.org/10.48550/arXiv.1709.04394

Wermiński, M., Perzyński K., Sitko M., & Madej Ł. (2023). Evaluation of data transfer influence in coupled Monte Carlo finite element model on microstructure evolution predictions. In L. Madej, M. Sitko, K. Perzynski (Eds.), *Material Forming: ESAFORM 2023. The 26th International ESAFORM Conference on Material Forming – ESAFORM 2023 – held in Kraków, Poland, April 19–21, 2023* (pp. 1551–1558). Materials Research Forum. https://doi.org/10.21741/9781644902479-167

Wermiński, M., Sitko M., & Madej Ł. (2025). Reducing the influence of the computational domain discretisation on grain growth in the cellular automaton austenite-to-ferrite transformation model. In P. Carlone, L. Filice, D. Umbrello (Eds.), *Material Forming: ESAFORM 2025. The 28th International ESAFORM Conference on Material Forming – ESAFORM 2025 – Paestum, Italy, 7–9 May, 2025* (pp. 1953–1961). Materials Research Forum. https://doi.org/10.21741/9781644903599-210

Williamson, A., & Delplanque, J.-P. (2015). Strain energy limitations in Monte Carlo Potts modeling of grain growth. *Computational Materials Science*, *108*(A), 48–55. https://doi.org/10.1016/j.commatsci.2015.05.032

Wolfram, S. (1984). Universality and complexity in cellular automata. *Physica D: Nonlinear Phenomena*, *10*(1–2), 1–35. https://doi.org/10.1016/0167-2789(84)90245-8

Wright, S. A., Plimpton, S. J., Swiler, T. P., Fye, R. M., Young, M. F., & Holm, E. M. (1997). *Potts-model grain growth simulations: Parallel algorithms and applications* (no. SAND97–1925). Sandia National Laboratories. https://doi.org/10.2172/522745

Wu, H. (2022). A review on the Cahn–Hilliard equation: Classical results and recent advances in dynamic boundary conditions. *Electronic Research Archive*, *30*(8), 2788–2832. https://doi.org/10.3934/era.2022143

Xiao, N., Tong, M., Lan, Y., Li, D., & Li, Y. (2006). Coupled simulation of the influence of austenite deformation on the subsequent isothermal austenite–ferrite transformation. *Acta Materialia*, *54*(5), 1265–1278. https://doi.org/10.1016/j.actamat.2005.10.055

Xu, Z., & Meakin, P. (2008). Phase-field modeling of solute precipitation and dissolution. *The Journal of Chemical Physics*, *129*(1), 014705. https://doi.org/10.1063/1.2948949

Yamanaka, A. (2023). Phase-field modeling and simulation of solid-state phase transformations in steels. *ISIJ International*, *63*(3), 395–406. https://doi.org/10.2355/isijinternational.ISIJINT-2022-343

Zhang, Jiantao, Hu, X., & Chou, K. (2020). In-situ environmental transmission electron microscopy investigation of the phase transformation austenite → ferrite in duplex stainless steel. *Materials Letters*, *264*, 127259. https://doi.org/10.1016/j.matlet.2019.127259

Zhang, Jin, Chadwick, A. F., Chopp, D. L., & Voorhees, P. W. (2023). Phase field modeling with large driving forces. *Npj Computational Materials*, *9*(1), 166. https://doi.org/10.1038/s41524-023-01118-0

Zhang, L., Zhang, C. B., Wang, Y. M., Wang, S. Q., & Ye, H. Q. (2003). A cellular automaton investigation of the transformation from austenite to ferrite during continuous cooling. *Acta Materialia*, *51*(18), 5519–5527. https://doi.org/10.1016/S1359-6454(03)00416-6

Zhang, X., Chen, J.-S., & Osher, S. (2008). A multiple level set method for modeling grain boundary evolution of polycrystalline materials. *Interaction and Multiscale Mechanics*, *1*(2), 191–209. https://doi.org/10.12989/IMM.2008.1.2.191

Zhang, Z., Ge, P., Li, J. Y., Ren, D. X., & Wu, T. (2022). Monte Carlo simulations of solidification and solid-state phase transformation during directed energy deposition additive manufacturing. *Progress in Additive Manufacturing*, *7*(4), 671–682. https://doi.org/10.1007/s40964-021-00253-8

Zheng, C., Raabe, D., & Li, D. (2012). Prediction of post-dynamic austenite-to-ferrite transformation and reverse transformation in a low-carbon steel by cellular automaton modeling. *Acta Materialia*, *60*(12), 4768–4779. https://doi.org/10.1016/j.actamat.2012.06.007

Zhi, Y., Jiang, Y., Ke, D., Hu, X., & Liu, X. (2024). Review on cellular automata for microstructure simulation of metallic materials. *Materials*, *17*(6), 1370. https://doi.org/10.3390/ma17061370

Zyska, A., Boroń, K., & Kordas, P. (2018). Modeling of dendritic structure evolution during solidification of Al-Cu alloy. *Archives of Foundry Engineering*, *18*(4), 87–92. https://doi.org/10.24425/afe.2018.125174